Exercise training enhances muscle mitochondrial metabolism in diet-resistant obesity

Chantal A. Pileggi,[a,b,c] Denis P. Blondin,[a,1] Breana G. Hooks,[a,b,d] Gaganvir Parmar,[a,b] Irina Alecu,[a,b] David A. Patten,[a,b] Alexanne Cuillerier,[e] Conor O'Dwyer,[a] A. Brianne Thrush,[a,2] Morgan D. Fullerton,[a,d,f] Steffany AL Bennett,[a,b,f] Éric Doucet,[g] François Haman,[g] Miroslava Cuperlovic-Culf,[a,b,c] Ruth McPherson,[h] Robert R.M. Dent,[i] and Mary-Ellen Harper[a,b,d]*

[a]Department of Biochemistry, Microbiology and Immunology, Faculty of Medicine, University of Ottawa, Ottawa, Ontario, Canada
[b]Ottawa Institute of Systems Biology, Ottawa, Ontario, Canada
[c]National Research Council of Canada, Digital Technologies Research Centre, Ottawa, Canada
[d]Centre for Infection, Immunity and Inflammation, Ottawa, Ontario, Canada
[e]Department of Cellular and Molecular Medicine, Faculty of Medicine, University of Ottawa, Ottawa, Ontario, Canada
[f]Centre for Catalysis Research and Innovation, Ottawa, Ontario, Canada
[g]School of Human Kinetics, Faculty of Health Sciences, University of Ottawa, Ottawa, Ontario, Canada
[h]Division of Cardiology, University of Ottawa Heart Institute, Ottawa, Ontario Canada
[i]Division of Endocrinology, Department of Medicine, University of Ottawa, Ottawa, Ontario, Canada

eBioMedicine 2022;83: 104192
Published online 11 August 2022
https://doi.org/10.1016/j.ebiom.2022.104192

Summary

Background Current paradigms for predicting weight loss in response to energy restriction have general validity but a subset of individuals fail to respond adequately despite documented diet adherence. Patients in the bottom 20% for rate of weight loss following a hypocaloric diet (diet-resistant) have been found to have less type I muscle fibres and lower skeletal muscle mitochondrial function, leading to the hypothesis that physical exercise may be an effective treatment when diet alone is inadequate. In this study, we aimed to assess the efficacy of exercise training on mitochondrial function in women with obesity with a documented history of minimal diet-induced weight loss.

Methods From over 5000 patient records, 228 files were reviewed to identify baseline characteristics of weight loss response from women with obesity who were previously classified in the top or bottom 20% quintiles based on rate of weight loss in the first 6 weeks during which a 900 kcal/day meal replacement was consumed. A subset of 20 women with obesity were identified based on diet-resistance (n=10) and diet sensitivity (n=10) to undergo a 6-week supervised, progressive, combined aerobic and resistance exercise intervention.

Findings Diet-sensitive women had lower baseline adiposity, higher fasting insulin and triglycerides, and a greater number of ATP-III criteria for metabolic syndrome. Conversely in diet-resistant women, the exercise intervention improved body composition, skeletal muscle mitochondrial content and metabolism, with minimal effects in diet-sensitive women. In-depth analyses of muscle metabolomes revealed distinct group- and intervention- differences, including lower serine-associated sphingolipid synthesis in diet-resistant women following exercise training.

Interpretation Exercise preferentially enhances skeletal muscle metabolism and improves body composition in women with a history of minimal diet-induced weight loss. These clinical and metabolic mechanism insights move the field towards better personalised approaches for the treatment of distinct obesity phenotypes.

Abbreviations: DR, diet-resistant with obesity; DS, diet-sensitive with obesity; ETC, electron transport chain; FFM, fat-free mass; IMTG, intramuscular triglycerides; OXPHOS, oxidative phosphorylation; RER, respiratory exchange ratio; ROS, reactive oxygen species; UCP3, uncoupling protein 3 3KS, 3-keto-sphinganine; CDase, ceramidase; CerS, ceramide synthase; CGT, ceramide galactosyltransferase; CerK, ceramide kinase; DAG, diacyl-glycerol; DES, desaturase; GalTase, galactosyltransferase; GCase, glucocerebrosidase; GCS, glucosylceramide synthase; GPC, glycerophosphocholine; GPE, glycerophosphoethanolamine; HexCer, hexosylceramide; Pase, phosphatase; S1P, sphingosine 1-phosphate; SK, sphingosine kinase; SM, sphingomyelin; SMase, sphingomyelinase; SMS, sphingomyelin synthase

*Corresponding author at: Department of Biochemistry, Microbiology & Immunology, Faculty of Medicine, University of Ottawa, 451 Smyth Rd, Ottawa, Ontario K1H 8M5, Canada.
E-mail address: mharper@uottawa.ca (M.-E. Harper).

[1] Current address: Division of Neurology, Department of Medicine, Faculty of Medicine and Health Sciences, Université de Sherbrooke and Centre de recherche du Centre hospitalier universitaire de Sherbrooke, Sherbrooke, Quebec, Canada.

[2] Current address: Clinical Epidemiology Program, Ottawa Hospital Research Institute, Ottawa, Ontario, Canada.

Funding Canadian Institutes of Health Research (CIHR-INMD and FDN-143278; CAN-163902; CIHR PJT-148634).

Keywords: Obesity; Muscle physiology; Mitochondria; Weight loss; Uncoupling; Mitochondrial supercomplexes; Metabolomics; Exercise; Serine; Sphingolipids

Research in context

Evidence before this study

The aim of the weight loss phase of most clinical weight management programs is to induce negative energy balance primarily through the prescription of hypocaloric diets. However, subsets of program-adherent individuals fail to achieve expected degrees of weight loss, even in intensively supervised weight loss programs. We have previously demonstrated that individuals with impaired weight loss exhibit profoundly different skeletal muscle characteristics as compared to age- sex- and initial body weight- matched patients who achieve weight loss success.

Added value of this study

By mining clinical data from over 5000 clinical records, we show that female patients who exhibit impaired weight loss have lower body (gynoid) adiposity. Conversely, those who achieve high degrees of diet-induced weight loss exhibit visceral (android) adiposity and are at greater risk for metabolic diseases. Remarkably, we also demonstrate that exercise training preferentially decreases fat mass and adiposity, and improves skeletal muscle bioenergetic function in women with a diet-resistant phenotype. Using extensive bioinformatics and machine learning approaches to analyse the metabolome and sphingolipidome of skeletal muscle, we establish mechanisms that could explain the greater benefits of exercise in diet-resistant obesity.

Implications of all the available evidence

Taken together, these findings confirm and substantially extend the notion of highly variable metabolic phenotypes in obesity that mandate personalised obesity therapies. In particular, exercise should be prioritised in patients resistant to diet-induced weight loss.

Introduction

The obesity epidemic is a major public health burden and is associated with multiple cardiometabolic comorbidities and an increased risk of all-cause mortality.[1] The cause of obesity is primarily attributed to a sustained positive energy balance combined with genetic, environmental, and behavioural factors that result in slow-progressing increases in body weight and adiposity.[2] Weight loss treatments aim to induce negative energy balance and commonly focus on decreasing energy intake through medically supervised low-calorie diet programs. Additional treatment strategies include behavioural and exercise interventions, a limited repertoire of approved prescription medications, and various types of bariatric surgery. Weight loss in response to these treatments often yields a notable variation in success, which is frequently attributed to a lack of adherence to prescribed treatments.[3,4] However, variations in weight loss capacity still exist even after controlling for adherence.[4,5] As such, determining the complex factors that influence interindividual weight loss success could improve outcomes for individuals with obesity that does not respond well to diet-induced weight loss interventions.

Diminished weight loss capacity is thought to be an evolutionarily conserved adaptation in energy expenditure that compensates for prolonged energy deficits.[6–9] The underlying mechanisms that drive these adaptations in energy-expenditure and weight loss susceptibility have been associated with differences in hormonal mediators,[10] tissue and cellular bioenergetics,[7,11,12] and genetic factors.[13–15] Skeletal muscle is a major site of metabolic activity accounting for ~20% of resting metabolic rate and representing 40–50% of total body weight. Therefore, identifying differences within skeletal muscle metabolism that lead to resistance or sensitivity in weight loss capacity could be key to understanding individual variations in weight loss response. Our group has demonstrated that diet-adherent individuals who lose weight rapidly in a clinically supervised hypocaloric meal-replacement program have several advantageous differences in skeletal muscle size, composition, and metabolism that could enhance capacity for weight loss. Specifically, muscle from diet-adherent patients in the top 20% for rate of weight loss (ROWL) (diet-sensitive; DS) have increased oxidative type I muscle fibres, higher mitochondrial proton leak, a greater antioxidant capacity, and increased expression of genes involved in glucose and fatty acid metabolism compared to patients in the bottom 20% who lose weight slowly in response to caloric restriction (diet-resistant; DR).[11,12,16,17] Here,

we aimed to assess the efficacy of exercise training on body composition and mitochondrial function in women with obesity identified as diet-resistant or diet-sensitive. Based on integrative approaches spanning from clinical databases to omics analyses in plasma and muscle, we report that the diet-sensitive phenotype is associated with factors that increase risk of metabolic disease, and that exercise training preferentially improves body composition, mitochondrial bioenergetics, skeletal muscle metabolism, and primary muscle cell oxidative capacity in DR women with obesity.

Methods

Review of patient records

Participants were previously classified into quintiles based on rate of weight loss (ROWL) calculated using serial measures in the first 6 weeks of a 26-week program, in which a 900 kcal/day meal replacement (Optifast 900; Nestlé Health Sciences) was consumed.[11] Comprehensive adherence to the Ottawa Hospital Weight Management Program (OHWMP) was determined as previously described,[11,16] where only diet-adherent women who had previously completed the OHWMP were strictly classified into quintiles based on ROWL classification by software developed by the clinic.[18] In brief, patients were excluded from quintile characterisation in the OHWMP and further metabolic studies if: they did not meet the adherence criteria; they were absent for >2 visits during the initial 6 weeks on meal replacement; physician notes expressed reservations about self-reported compliance; and/or there was inadequate completion of the laboratory testing protocol. Records of highly adherent women (BMI 30−50 kg/m^2, age 30−60 y, weight) were screened for eligibility by quintile (top 20%, diet-sensitive (DS), and bottom 20%, diet-resistant (DR)), and missing/incomplete data. 228 DR and DS patient records were paired based on age (±5 years), weight (±10 kg), and BMI (±3.5 kg/m^2) for analyses, resulting in 114 pairs.

Evaluation of body composition. Serial measurements of body composition were taken weekly on patients enrolled in the OHWMP using bioimpedance analysis (BIA; Tanita Corporation, Arlington Heights, IL). A subset of 40 patients were recruited for body composition analysis by dual x-ray absorptiometry (DEXA; GE Lunar, Prodigy Model).

Exercise intervention

Exercise intervention subject details and sample size calculation. Program adherent women from the OHWMP were contacted to participate in a supervised exercise intervention. Participants were screened prior to enrolment and excluded from the study for prior bariatric surgery and medications known to affect weight loss including: medications that affect glucose homeostasis, appetite suppressants, steroids, and/or medications/supplements that may affect muscle biology. All participants were non-smokers, and free from pathologies such as diabetes, cardiovascular disease, cancer, and musculoskeletal conditions that result in impaired movement. We previously showed that the characteristic feature between individuals who have obesity and sensitive vs. resistant to a very-low calorie nutritional intervention is a significant inter-group difference in non- phosphorylating (state 4) mitochondrial respiration, also referred to as mitochondrial proton leak[11] (effect size =1.24, SD=48−52 nmol·min^{-1}·mg protein-1, n=12). To ensure that our cohort exhibited the same characteristic features before beginning the exercise intervention, we calculated that 12 participants would be required for a power > 80%, at a two-sided alpha level of 0.05 or at least 10 participants for a power >90%, at a one-sided alpha level of 0.10.

Nine DS and 9 DR women were matched at the time of enrolment for age (±5 years), body mass (±20 kg) and BMI (±3.5 kg/m^2). One additional pair of women were matched based on age and BMI, but not body mass (for a total of n=10 DS, n=10 DR). The participants were instructed to maintain their normal lifestyle and eating habits. Subjects underwent a muscle biopsy and exercise testing (detailed below) before and after the exercise intervention (Figure 2a).

Exercise intervention study design. The exercise intervention consisted of 18-supervised progressive exercise sessions performed 3 times per week on non-consecutive days for six weeks. Each exercise session consisted of 30 minutes of treadmill walking followed by a resistance-based circuit. Participants performed the treadmill walking at the same relative workload of six metabolic equivalents (METs) at week 1 (estimated from the treadmill test), which increased by 10% weekly. However, the absolute workload was ~25% higher in DS women than DR (6 METs for DS=1.85±0.49 L of O_2·min^{-1}, DR=1.49±0.21L of O_2·min^{-1}; P=0.047, t-test). Following the treadmill walk, participants completed three sets (eight to twelve repetitions per set) of resistance-based exercises and one core exercise at 60−80% of their predicted one-repetition maximum.[19]

Assessment of physical activity. Self-reported physical activity was determined using an approved questionnaire with a 5-point Likert scale with a value of 1 defined as an "inactive" (e.g., seated almost exclusively) and a value of 5 defined as a "very active" (e.g., walking nearly continuously). Participants were instructed to maintain their typical physical activity throughout the study.

Physical activity was monitored with a wrist-worn accelerometer (Fitbit Charge, San Francisco, CA) to track levels of activity throughout the study.

Evaluation of body composition. Body weight was measured in light clothing to the nearest 0.010 kg. Height was determined using a wall-mounted stadiometer. Body composition was assessed by DEXA (GE Lunar, Prodigy Model). Daily calibration procedures were performed according to manufacturer's instructions. DEXA scans were analysed by a single blinded-operator.

Participants reported to the University of Ottawa Behavioural and Metabolic Research Unit. Resting metabolic rate was measured in the morning, following a minimum 10–12 h overnight fast using a flow-through open circuit respirometry system with a ventilated hood (Field Metabolic System, Sable Systems International, Las Vegas, NV, USA) while participants rested quietly in a semi-supine position for 60 min at ambient temperature. Whole-body RMR and substrate utilisation were calculated using the rates of oxygen consumption and carbon dioxide production, as described previously.[20]

Participants performed a graded submaximal treadmill test to determine the incremental increase in energy expenditure in response to increasing workloads. After a 3-min warm-up at 5 W, the workload was increased by 20 W every 3 min for 4–5 stages. Oxygen consumption and carbon dioxide production were measured continuously throughout the exercise period using a flow-through open circuit respirometry system with a mask (Field Metabolic System, Sable Systems International, Las Vegas, NV, USA). These data were then used to determine the starting workloads for the exercise sessions. Heart rate was also collected continuously throughout the exercise period, and perceived exertion was recorded every 3 min using the Borg scale.[21] Substrate utilisation and energy expenditure were calculated using the rates of oxygen consumption and carbon dioxide production, as described previously.[20]

Muscle function. Muscle function was determined by maximal voluntary isometric contraction (MVC) and 1RM. Three 5 s unilateral knee extension MVCs were measured on a Biodex dynamometer (Shirley, NY) at a knee angle of 60° with 1 minute of rest between contractions. Predicted one repetition maximums were estimated using the Brzycki equation.[19]

Blood biochemistry. Blood samples were collected after an overnight fast, and routine analyses were carried out in the Clinical Biochemistry Laboratory at the Ottawa Hospital (Ottawa, Ontario, Canada).

Skeletal muscle sampling, tissue collection and preparation. V*astus lateralis* muscle biopsies were collected from fasting subjects using a Bergstrom needle modified for manual suction under local anaesthesia. Subjects were asked to refrain from physical activity for 48 h prior to the biopsy, with the post-exercise training (PET) biopsy collected 72 h following the last exercise session. The obtained sample was dissected clean from visual adipose and subsequently divided for analysis based on priority and tissue availability. One portion of tissue was placed in culture media for isolation of satellite cells, one portion was snap frozen in liquid nitrogen and stored at −80 °C for later analyses. If sample size permitted, one portion was OCT embedded and one portion was placed in ice-cold BIOPS for mitochondrial respiration analysis (BIOPS, pH 7.1 (5.77 mM Na_2ATP, 10 Ca-EGTA buffer (0.1 μM free Ca^{2+}) 6.56 mM $MgCl_2{\cdot}6H_2O$, 20 mM taurine, 60 mM K-lactobionate, 15 mM phosphocreatine, 20 mM imidazole, 0.5 mM DTT, 50 mM MES).

Fasting plasma biochemical analysis. Fasted blood samples were analysed by the Ottawa Hospital Laboratory Services. Homeostatic model assessment of insulin resistance (HOMA-IR) was calculated from fasting glucose and insulin concentrations.

Muscle fibre type and cross-sectional area. Muscle samples embedded in OCT were cut into 10 μm cross–sections at −20 °C on a cryostat and mounted on microscope slides. Air-dried cross-sections were blocked for 60 min in 10% goat serum with phosphate buffered saline (PBS) before incubation overnight at 4 °C in primary antibodies against type I myosin (mouse IgG2b; DSHB, BA–F8, RRID:AB_10572253, 1:50), type II myosin (mouse IgG1; DSHB, SC–71, RRID:AB_2147165, 1:300), and dystrophin (mouse IgG2a; DSHB, MANDYS1(3B7), RRID:AB_528206, 1:12.5).[22] The following morning, sections were washed in PBS and then incubated at room temperature for 60 min with the respective secondary antibodies at a 1:500 dilution in PBS (goat anti–mouse IgG1, Alexa Fluor 488 (Invitrogen, A-21121, RRID:AB_2535764) to detect SC–71; goat anti–mouse IgG2b, Alexa Fluor 350 (Invitrogen, A–21147, RRID:AB_2535777) to detect BA–F8; and goat anti–mouse IgG2a Alexa Fluor 647 (Invitrogen, A–21241, RRID:AB_2535810) to detect MANDYS1 (3B7)). Images were acquired on a Thermofisher FL Auto 2 microscope and analysed semi-automatedly using ImageJ software.

High resolution respirometry in permeabilised muscle fibres. High-resolution respirometry on saponin-permeabilised *vastus lateralis* was conducted using an Oxygraph-2k system with an attached fluorometer (OROBOROS Instruments, Innsbruck, Austria). Experiments were performed in duplicate at 37 °C in 2 mL of mitochondrial respiration media [MiR05 (in mM): 110

sucrose, 60 K-lactobionate, 20 HEPES, 20 taurine, 10 KH_2PO_4, 3 $MgCl_2$, 0.5 EGTA, and 1 mg/ml fraction V BSA, pH 7.1 at 37 °C]. H_2O_2 emission was determined simultaneously using 50 μM Amplex Ultra Red in the presence of 5 U/mL superoxide dismutase (SOD), and horseradish peroxidase (HRP). The assay protocol consisted of consecutive additions of: 2 mM malate, 5 mM pyruvate, 10 mM glutamate (CI substrates), 5 mM ADP (CI OXPHOS), 10 mM succinate (CI+II OXPHOS), 2.5 μM oligomycin (CI+II Leak), 0.5 μM titrations of carbonyl cyanide p-trifluoromethoxyphenyl hydrazine (FCCP) (maximal respiration, ETS) and 2.5 μM antimycin A. Values were adjusted for non-mitochondrial oxygen consumption (*i.e.,* that in the presence of AA), and expressed relative to tissue wet weight. Citrate synthase (CS)-normalised oxygen flux (pmol O_2/U/CS) was calculated to account for potential variations in mitochondrial mass.

Isolation of primary myoblasts. Satellite cells were isolated from *vastus lateralis* muscle and purified via immunomagnetic sorting using CD56 MicroBeads (Miltenyi Biotec). Myoblasts were cultured on Matrigel-coated dishes in Ham's F10 media supplemented with 15% BGS, 1% antibiotic-antimycotic, 2.5 μ/mL gentamycin, 826 nM dexamethasone, 8.3 ng/mL human epidermal growth factor, and 25 pmol of insulin. For differentiation into myotubes, cells were cultured in low glucose DMEM supplemented with 2% horse serum, 1% antibiotic-antimycotic, and 2.5 μ/mL gentamycin.

Seahorse analysis of cellular bioenergetics. Cellular bioenergetics was assessed with the Seahorse XFe96 Analyzer (Agilent). Myoblasts were plated at 15,000 cells/well onto Matrigel-coated Seahorse plates and differentiated in low glucose DMEM for 7 days. One hour prior to experimentation, cells were washed and incubated in HCO_3-free DMEM media supplemented with 4 mM l-glutamine, 1 mM Na-pyruvate and 5 mM D-glucose, pH 7.4. Myotubes were treated with sequential injections of oligomycin [2 μg/mL], FCCP [2 μM], antimycin A [1 μM] with rotenone [1 μM], and monensin [20 μM]. Following completion of the assay, Seahorse XF Media was removed, and cells were washed with PBS followed by lysis with RIPA Lysis Buffer (0.5 M Tris-HCl, pH 7.4, 1.5 M NaCl, 2.5% deoxycholic acid, 10% NP-40, 10 mM EDTA). The amount of protein per well was determined by the BCA assay method using the Pierce™ BCA Protein Assay Kit (Thermofisher, 23225). Bioenergetic capacity and fuel flexibility were investigated by graphing glycolytic and oxidative ATP production as previously described.[23]

Immunofluorescence of primary myoblast mitochondrial length. Primary myoblasts seeded on coverslips were fixed with 4% paraformaldehyde. Mitochondrial length was determined by staining with TOM20 (Santa Cruz Biotechnology, sc-11415, RRID:AB_2207533, 1:100) in PBS buffer containing 0.1% Triton X-100 and 1% BSA. Goat anti-rabbit (H+L) secondary antibody, Alexa Fluor 488 (Thermofisher, A-11008, RRID:AB_143165, 1:100) was diluted in 1x PBS containing Hoechst counter-stain. Images were obtained using a Zeiss Axiolimager Z1 microscope. Blinded analysis was conducted by quantifying 50 mitochondrial lengths from 3 to 5 fields of view.

Protein extraction. Frozen muscle was homogenised using a bead mill homogeniser (Fisherbrand Bead Mill 24 Homogenizer) in ice-cold RIPA buffer (Millipore) supplemented with 0.5 mM Na_3VO_4 and protease inhibitor cocktail (Sigma). Protein concentration was determined using a commercially available bicinchoninic acid kit according to the manufacturer's protocol (Thermofisher).

Immunoblotting. Proteins were separated by SDS-PAGE under reducing conditions and transferred to PVDF membranes and incubated overnight with primary antibodies against: PGC1α (Millipore, ST1202, RRID:AB_2237237, 1:1000), ANT (Santa Cruz Biotechnology, sc-9299, RRID:AB_671086, 1:2000), UCP3 (Abcam, ab3477, RRID:AB_2304253, 1:2000), SPTLC1 (Proteintech, 15376-1-AP, RRID:AB_2286678, 1:1000) SPTLC2 (Proteintech, 51012-2-AP, RRID:AB_2195870, 1:1000), and vinculin (Abcam, ab129002, RRID: AB_11144129, 1:5000). Protein bands were visualised using the ChemiDoc™ MP Imaging System (Bio-Rad). Densitometry band analysis was performed using Image J software. Abundance of target proteins are presented normalised to vinculin.

Enzyme activities. Enzymatic activities for citrate synthase (CS) and succinate dehydrogenase (SDH) were performed using the BioTek Synergy Mx Microplate Reader (BioTek Instruments, Inc., Winooski, VT) as previously described.[24] Briefly, CS activity was determined by measuring absorbance at 412 nm in 50 mM Tris-HCl (pH 8.0) with 0.2 mM DTNB, 0.1 mM acetyl-CoA and 0.25 mM oxaloacetate SDH activity was determined by measuring the reduction of dichlorophenolindophenol (DCPIP) through decreased absorbance at 600 nm at 25 mM potassium phosphate buffer (pH 7.5), 20 mM succinate, 80 μM DCPIP, 50 μM decylubiquinone, 1 mg/ml FAF-BSA, and 300 μM KCN. Rate of change of absorbance and pathlength of each well were determined and enzyme activities were calculated using extinction coefficients of ε=13.6 $mM^{-1}cm^{-1}$ for CS and ε=19.1 for SDH.

Mitochondrial supercomplex analysis. *Vastus lateralis* samples were assessed for ETC supercomplexes by blue native PAGE (BN−PAGE). Samples were minced and

dounce homogenised on ice in sucrose buffer (250 mM sucrose, 20 mM imidazole/HCl, pH 7.0) and centrifuged for 10 min at 10,000 xg. The membrane fraction containing mitochondria was then resuspended in extraction buffer [50 mM imidazole/HCl pH 7.0, 50 mM NaCl, 5 mM 6−aminohexanoic acid, 1 mM EDTA with 1.5% w/v digitonin (experimentally determined, final digitonin to tissue ratio of 1:10 w/w)], and gently solubilized with agitation for 30 min, and then subsequently cleared by centrifugation 30 min at 14,000 xg. Myotube pellets assessed for ETC supercomplexes were resuspended in extraction buffer with 1.5% w/v digitonin, followed by gentle solubilization with agitation for 30 min, and then subsequently cleared by centrifugation for 30 min at 14,000 xg.

The supernatant containing solubilized membrane proteins for both muscle homogenate and primary myotubes were mixed with glycerol (5% v/v final) and 5% Coomassie blue G-250 solution to achieve a 1:4 dye:digitonin ratio. Samples were separated on 3−13% gradient gels and then transferred to nitrocellulose membrane. Membranes were probed using the following primary antibodies: NADH dehydrogenase (ubiquinone) 1α subcomplex subunit 9, mitochondrial (NDUFA9; Thermofisher, 459100, RRID:AB_2532223, 1:2000), complex II (Fp) succinate dehydrogenase complex, subunit A, flavoprotein variant (SDHA; Thermofisher, 459200, RRID:AB_2532231, 1:20000), complex III ubiquinol−cytochrome c reductase core protein II, (UQCRC2; Abcam, ab14745, RRID: AB_2213640, 1:2000); complex IV (subunit I) (MTCO1; Thermofisher, 459600, RRID: AB_2532240, 1:2000), and complex V (ATP synthase subunit a, mitochondrial) (ATP5A; Abcam, ab14748, RRID:AB_301447, 1:2000). ETC supercomplexes were analysed based on their banding pattern, as previously confirmed by 2D−BN−PAGE.[25]

Metabolite extraction from skeletal muscle and LC-MS analysis. Frozen *vastus lateralis* was quickly homogenised with using a bead mill homogeniser at 4 °C (Fisherbrand Bead Mill 24 Homogenizer) in −20 °C equilibrated solution containing methanol, water, and acetonitrile (OmniSolv, Sigma). Homogenates were then incubated with a 2:1 dichloromethane:water solution on ice for 10 min. The polar and non-polar phases were separated by centrifugation at 4000 xg for 10 min at 1 °C. The upper polar phase was dried using a refrigerated CentriVap Vacuum Concentrator at −4 °C (LabConco Corporation, Kansas City, MO). Samples were resuspended in water and run on an Agilent 6470A tandem quadrupole mass spectrometer equipped with a 1290 Infinity II ultra-high performance LC (Agilent Technologies) utilising the Metabolomics Dynamic MRM Database and Method (Agilent), which uses an ion-pairing reverse phase chromatography.[26] This method was further optimised for phosphate-containing metabolites with the addition of 5 µM InfinityLab deactivator (Agilent) to mobile phases A and B, which requires decreasing the backflush acetonitrile to 90%. Multiple reaction monitoring (MRM) transitions were optimised using authentic standards and quality control samples. Metabolites were quantified by integrating the area under the curve of each compound using external standard calibration curves with Mass Hunter Quant (Agilent). No corrections for ion suppression or enhancement were performed, as such, uncorrected metabolite concentrations are presented.

Plasma amino acid analysis. Fasted plasma samples were extracted as previously described.[27] Briefly, samples were diluted 1:100 in 0.5 mM tridecafluoroheptanoic acid solution containing a commercially available internal standard solution (A9906, Sigma Aldrich). Liquid chromatography was performed using a Xevo TQD Tandem Mass Spectrometer (Water, Milford, MA), fitted with an ACCQ-TAG Ultra C18 1.7 um (2.1 × 100 mm) column.

Lipidomic analysis. Sphingolipids were extracted by a modified Bligh and Dyer method[28] as described in Granger et al. (2019).[29] Deuterated lipid standards were from Avanti Polar Lipids (Alabaster, USA) (Cer(d18:1/16:0-D31, GlcCer(d18:1/8:0), GalCer(d18:1/8:0), and SM (d18:1/18:1-D9)) and were added at the time of extraction. The chloroform phase containing the lipids was dried under a constant stream of nitrogen, and lipids were then re-solubilized in 300 µL of 100% ethanol, flushed with nitrogen, and stored at -80 °C.

The samples were analysed on an Agilent 1290 Infinity II liquid chromatography system coupled to a QTRAP 5500 triple quadrupole-linear ion trap mass spectrometer with Turbo V ion source (AB SCIEX, Concord, Canada). 5 µL of sample was loaded in 96-well plates in 2.5 µL of 100% ethanol and 16 µL of solvent A (water with 0.1% formic acid and 10 mm ammonium acetate). 3 µL of sample was picked up from the well and injected with the system operating at a flow rate of 10 µl/min. Reverse phase chromatography was performed using a 100 mm × 250-µm (inner diameter) capillary column packed with Reprosil-Pur 120 C8 and a binary solvent gradient with solvent A (described above) and solvent B consisting of acetonitrile and isopropanol in a ratio of 5:2 v/v with 10 mm ammonium acetate and 0.1% formic acid. Each sample ran for 50 min, with the gradient starting at 30% B and reaching 100% B at 5 min, which was maintained for another 30 min. The gradient then ramped down to 30% B for 1 min and remained at this composition until the end of the run to re-equilibrate the column. Data were acquired in positive ion mode using selected reaction monitoring (SRM), monitoring transitions from protonated

molecular ions with Q3 ions of either m/z 264.3 (sphingosine backbone) or 184.1 (phosphocholine head group).

The molecular identities of lipid species were confirmed through an information-dependent acquisition (IDA)-enhanced product ion (EPI) experiment, where EPI spectra were analysed for structural determination. Data acquisition was performed using Analyst software version 1.6.2 (AB SCIEX) and quantification analysis of SRM data was done in MultiQuant 3.0.2 software version 3.0.8664.0 (SCIEX). Raw peak areas were normalised to the appropriate internal standards to account for extraction efficiency and instrument response, as well as to the tissue wet weight.

Data mining and network analysis. Machine learning and network analysis were performed using Matlab 2021 (Matworks, Inc). Feature selection used ReliefF (command relief running under Matlab) and represented using in-house routines. Briefly ReliefF predicts classification rank, *i.e.,* within the group significance, for each feature.[30] This method ranks predictor features by weight and contribution to the regression to response vector (in this case 4 cohort groups). Negative weight indicates that feature is not a good predictor and large positive weight indicates an important predictor with feature weight depending on the level of difference between a given feature and other features in nearby instances of the same class relative to the instances of the other class. Feature selection was performed using Euclidean distances as a metric for feature similarity and 4 nearest neighbours were used for weight assessment.

Correlation analysis uses distance correlation calculation performed under Matlab using an in-house routine, based on the method presented by Szekely and Rizzo[31] with P-values calculated using Student's t cumulative distribution function (TCDF function in Matlab). Although distance correlation, by definition, provides only positive values, we have introduced signed distance correlation by deriving and associating correlation signs from Pearson correlation calculation. Distance correlation was calculated between all metabolites separately in four groups.

Determinations of functional features and metabolite changes between subject groups were based on the network results and obtained using linear regression comparisons between the two groups for each metabolite, comparing values of edges to all other metabolites between the two groups. Linear regression comparisons were performed between distance correlations for each metabolite with all other metabolites calculated for each subject cohort. The level of change is reported as a slope of linear regression. The major changes were identified as the largest divergences from the slope of 1 that would be obtained for the identical trends in correlations.

Ethics

All participants provided informed oral and written consent. This study was approved by the Ottawa Health Science Network Research Ethics Board (Protocol #1998133-01H and #2011658) and the University of Ottawa Council of Research Ethics Board (Protocol #H01-12-06).

Statistical analysis

Statistical analysis was performed using SigmaPlot for Windows version 14.5 (Systat Software Inc., San Jose, CA). Statistical significance of DS *vs* DR was determined using a two-tailed Student's t-test. To assess the effect of the exercise intervention between DS and DR, a two-way ANOVA with repeated measures with exercise as a repeated factor and ROWL quintile (DS/DR) as a between-subjects factor was used with Holm-Sidak post hoc tests. While the participants were matched at the time of recruitment to balance patient characteristics that have been associated with rate of weight loss, a matched study analysis was not used for the statistical analysis of the data given that sample availability rendered us unable to perform some molecular analyses from all the participants. Data were checked for normality of the residual error distribution and $\log_{10}$ transformed where appropriate. Statistical differences were considered significant when the P value was <0.05. Prism software (GraphPad Software Inc., La Jolla, California, USA) was used to generate graphs. Data are presented as means±SD unless otherwise specified.

Role of funders

This work was supported by the Canadian Institutes of Health Research. The funder had no influence on the conceptualisation, data collection, analysis, or interpretation of data presented within the manuscript.

Results

Diet-sensitive obesity is associated with visceral adiposity and greater cardiometabolic risk

Differences in ROWL in highly-adherent individuals were previously reported as part of an intensively supervised clinical weight loss program in which a cohort of over 5000 patients with obesity followed a 6-week hypocaloric meal replacement of 900 kcal/day with intensive weekly supervision and educational programming.[11] We have shown that ROWL varies ~2–3 fold between DS and DR patients with obesity after controlling for factors currently known to affect weight loss, including thyroid function, specific medications and pathologies, obesity-related surgeries, and mobility issues. Here, we began by reviewing patient records prior to the start of the hypocaloric meal replacement diet to identify characteristics that might predict differences in ROWL. The 228

patient records that were included in the review are reflective of the female population in the OHWMP (Figure 1a). We included women with BMI 30−60, and age 30−70, as based on our own observations, that is when rate-of-weight-loss is consistently stable. We acknowledge that there are multiple socio-economic parameters that may cause barriers for certain demographics to not seek medical care for obesity treatment, however, this was not examined in this study.

In a subset of 228 DS and DR women with obesity matched based on age, weight, and BMI (Figure 1a), 213 were of European descent (93.4%), 4 were of African descent (1.8%), 2 were of Asian descent (0.9%), 7 were other (3%), and 2 were unknown (0.9%). Bioelectrical impedance analysis (BIA) of body composition revealed that initial body fat (%) was higher in DR individuals compared to DS ($P<0.01$, two-tailed Student's t-test, Table S1, Figure 1b). However, waist circumference, which is highly correlated with visceral adipose tissue,[32] was higher in DS women ($P<0.05$, two-tailed Student's t-test, Figure 1c). Visceral adipose tissue is preferentially lost in subjects with obesity on a low calorie diet as intraabdominal adipocytes readily undergo lipolysis.[33] Supporting this, DS women also exhibited a higher rate of fat mass loss throughout the weight loss program compared to DR women ($P<0.01$ and $P<0.001$ respectively, two-tailed Student's t-test, Figure 1e and 1f).

Blood biochemistry profiles revealed that DS individuals had higher fasting insulin concentrations (Figure 1d), higher HOMA-IR, elevated triglycerides (TG), and lower levels of TSH and HDL cholesterol ($P<0.05$ for all, two-tailed Student's t-test, Table S1). While all DR and DS women had TSH values within normal range, even small elevations in TSH are associated with the increased occurrence of obesity.[34] The higher waist circumference, fasting insulin, HOMA-IR and TGs in DS women suggest that women with obesity who lose weight rapidly in response to diet restriction may be at greater risk of metabolic syndrome (MS). Therefore, we next assessed the prevalence of MS using the ATP-III criteria.[35] DS women had a greater number of ATP-III MS criteria compared to DR women ($P<0.01$, two-tailed Student's t-test, Table S1), indicating that DS obesity may confer a greater risk for cardiometabolic disease.

BIA accuracy is influenced by factors such as hydration status, patient ethnicity, hormonal fluctuations, and tends to underestimate fat mass and overestimate lean mass in individuals with obesity.[36] Thus, we next sought to confirm the differences in body composition between DR and DS women by dual-energy X-ray absorptiometry (DEXA) in 20 matched pairs. Consistent with our BIA data, DR individuals with obesity had a greater body fat (%) compared to DS women ($P<0.001$, two-tailed Student's t-test, Figure 1g). Interestingly, DR women exhibited less lean body mass compared to DS women ($P<0.05$, two-tailed Student's t-test, Figure 1h and 1i). Regional analysis of fat distribution revealed that android fat (%) did not differ between groups, but DR women had greater gynoid and leg fat (%) compared to DS women ($P<0.01$ and $P<0.001$ respectively, two-tailed Student's t-test, Figure 1j and 1k, Table S1). These regional differences resulted in a lower ratio of android to gynoid fat in DR women ($P<0.05$, two-tailed Student's t-test, Figure 1l).

Exercise training improves body composition in diet-resistant women with low resting metabolism and muscle strength

Exercise has well recognised benefits to muscle function and structure that can enhance capacity for maintained weight loss and improve clinical prognosis.[37,38] Considering our findings of decreased FFM in DR women with obesity, as well as our previous findings of lower muscle cross-sectional area (CSA),[16] we hypothesised that a combined aerobic and resistance exercise training intervention may confer greater benefits to DR individuals. To test this hypothesis, we conducted a 6-week supervised, progressive, combined aerobic and resistance exercise intervention with 9 DS and 9 DR women matched at the time of enrolment for age, weight, and BMI, with an additional pair of 1 DS and 1 DR women matched for age and BMI but not weight (Figure 2a; details of the exercise protocol are provided in the Methods). The DS and the DR groups were similar with regard to age ($P=0.9$, two-tailed Student's t-test), weight ($P=0.2$, two-tailed Student's t-test) and BMI ($P=0.7$, two-tailed Student's t-test). However, despite similar levels of self-reported physical activity between groups ($P=0.6$, two-tailed Student's t-test, Table 1), accelerometer data revealed that DR women were walking on average 2000 fewer steps per day compared to DS women throughout the 6-week intervention (main effect of DS vs. DR $P<0.05$, two-way ANOVA for repeated-measures, Figure S1).

Consistent with our analysis of patient records from the cohort of 228 patients with obesity, DR women had higher body fat (%) and lower lean mass compared to DS prior to exercise training (group within BL $p<0.05$, two-way ANOVA for repeated-measures with Holm-Sidak post hoc test, Table 1). Plasma biochemistry analyses confirmed our findings of elevated fasting insulin (main effect of DS vs. DR $P<0.05$, two-way ANOVA for repeated-measures, Table 1), and revealed that DS women had higher creatine kinase (main effect DS vs. DR $P<0.01$, two-way ANOVA for repeated-measures), indicative of greater muscle mass.

Analysis of resting metabolic rate by indirect calorimetry revealed ~20% lower energy expenditure in DR women compared to DS women at BL (group within BL $P<0.05$, two-way ANOVA for repeated-measures with Holm-Sidak post hoc test, Figure 2c, Table 1). Since RMR is positively correlated with lean body mass and

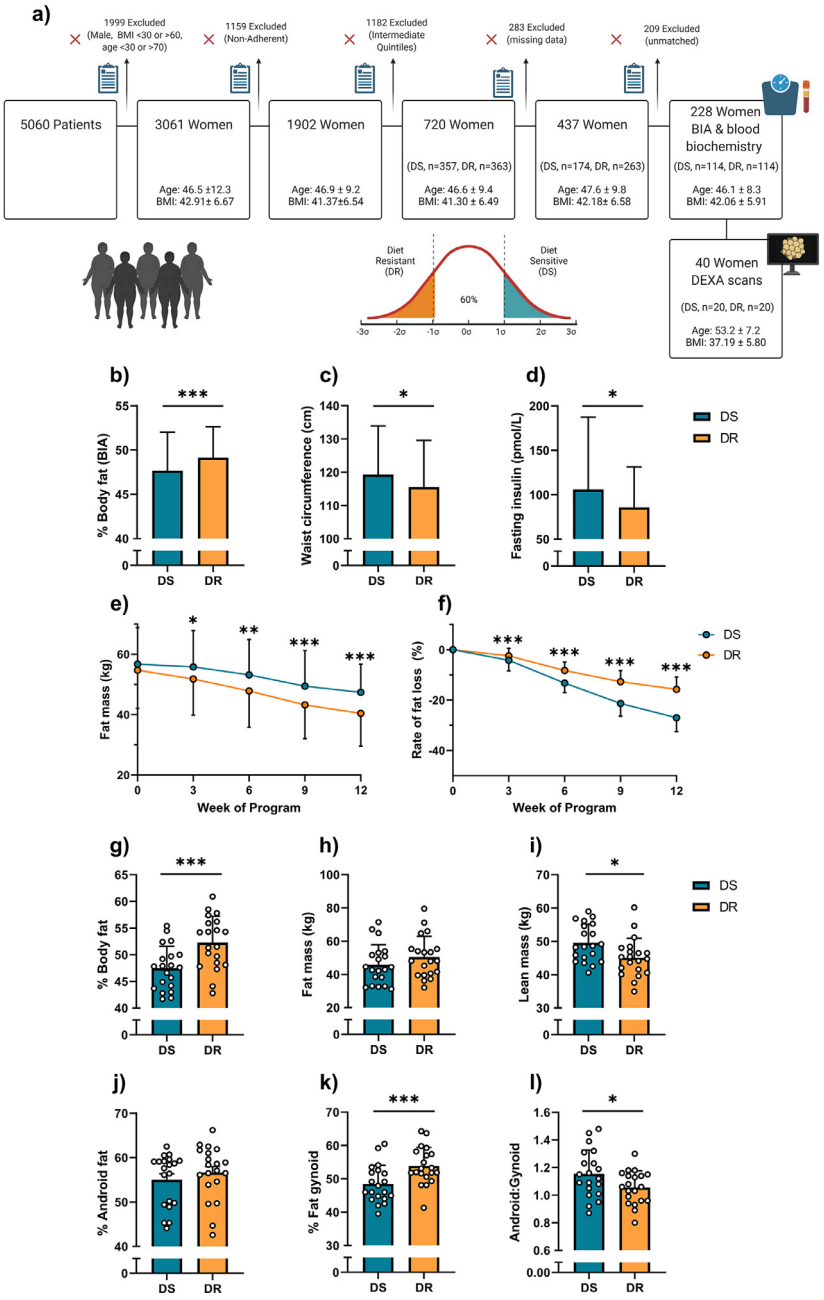

Figure 1. Diet-sensitive women with enhanced weight loss capacity have lower body fat (%), but are more at risk of cardiometabolic diseases associated with obesity. (a) Summary of screening patient records for eligibility. Patient records from the Ottawa Hospital Weight Management Clinic were assessed for adherence (as previously described), and screened for missing data. Records from patients with obesity in the top 20% for weight loss success (diet-sensitive, DS) were reviewed and compared to well-matched women in the bottom 20% of rate of weight loss (diet-resistant, DR). **(b-d)** Body composition and blood biochemistry of 228 matched DS and DR women with obesity (n=114). **(b)** DR women have greater body fat (%) as assessed by bioelectrical impendence analysis (BIA). **(c)** DR women had a smaller waist circumference, and **(d)** lower fasting insulin compared to DS women with obesity. **(e-f)** DR women with obesity lost less fat mass in 12 weeks while on a 900 kcal/day hypocaloric diet. **(e)** Fat mass across 12-weeks; **(f)** Rate of fat mass loss. **(g-l)** Body composition analysed by DEXA of 40 well-matched DR and DS women with obesity, (n=20). **(g)** Body fat (%) was higher in DR women with obesity. **(h)** Fat mass was similar between groups, whereas **(i)** lean mass was lower in DR women. Regional analyses showed no difference between groups in android fat **(j)**, but revealed greater gynoid fat in DR women **(k)**. The regional differences in fat mass resulted in a higher ratio of android:gynoid fat in DS obesity **(l)**. Comparisons between groups were as determined using a two-tailed Student's t-test. *P<0.05, **P<0.01, *** P<0.001. Values are means±SD.

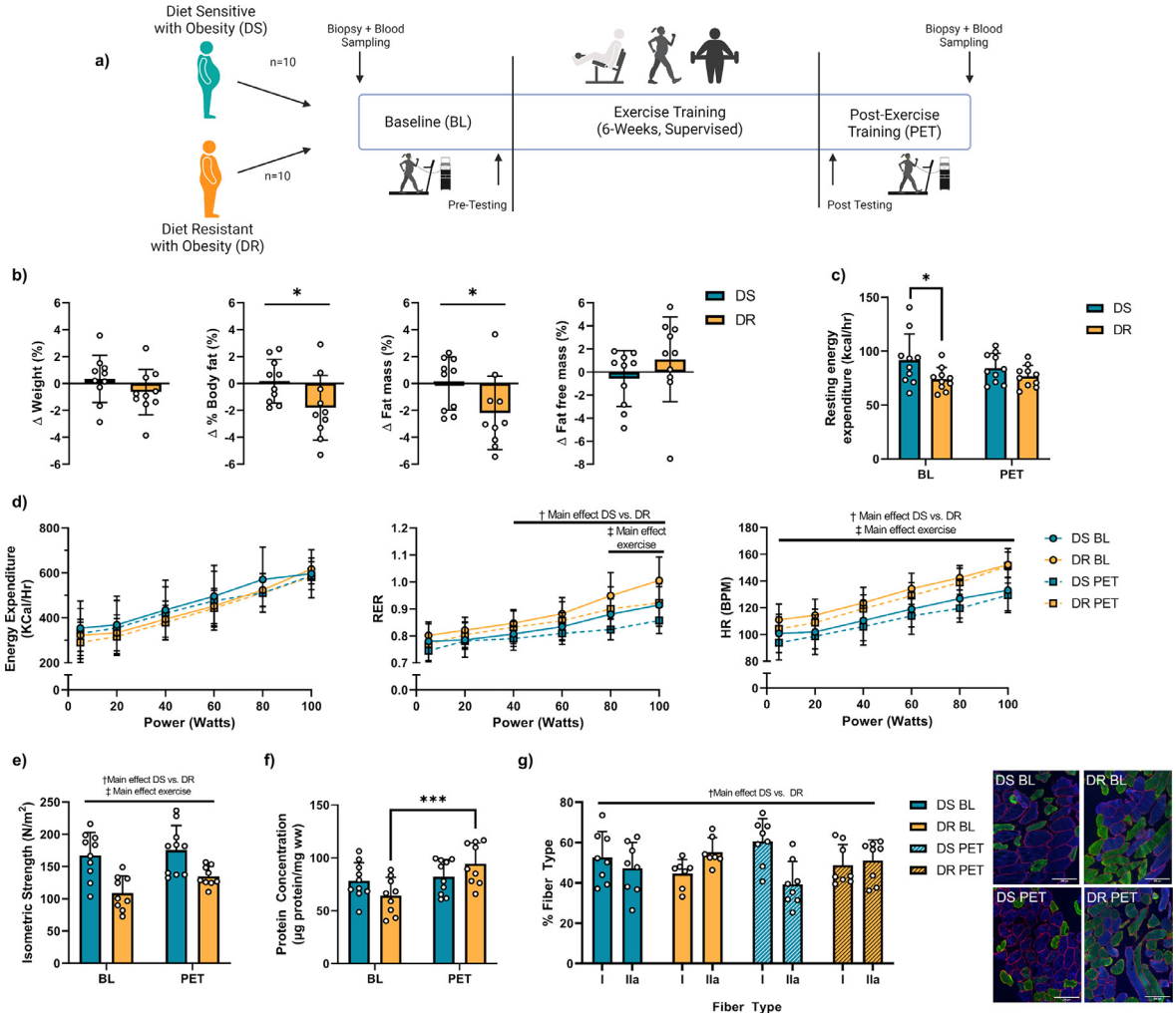

Figure 2. Exercise training preferentially improves body composition in diet-resistant women with low resting metabolism and muscle strength. (a) Schematic summary of the time points for sample collection, testing procedures, and intervention. Briefly, 10 diet-sensitive (DS) and 10 age-, weight-, and BMI-matched diet-resistant (DR) women with obesity were recruited to undergo a 6-week supervised exercise training intervention. Baseline (BL), post-exercise training (PET). **(b)** Exercise training did not induce weight loss or alter fat-free mass in either group, but selectively lowered body fat (%) and fat mass in DR women, (n=10, two-tailed Student's t-test *P<0.05). See also Table 1. **(c)** DR women had lower resting energy expenditure at BL compared to DS women with obesity, but not PET, (n=10). **(d)** DS and DR did not differ in energy expenditure during exercise when assessed using a graded submaximal exercise; However, DR women had a higher respiratory exchange ratio (RER) at greater workloads (40W), and higher heart rates (HR) throughout the exercise test. Exercise training lowered RER and HR in both groups, (n=10). **(e)** Isometric strength during knee extension was lower in DR women regardless of exercise training. Exercise training improved strength in both groups, (n=10 DS, n=9 DR). **(f)** Exercise training increased skeletal muscle protein concentration per mg tissue in DR women only, (n=9−10). **(g)** DR muscle exhibited fewer type I fibres than DS muscle, regardless of exercise training, (n=8 DS, n=7 DR). All values are presented as means ± SD. Unless otherwise stated, a two-way ANOVA for repeated-measures with Holm-Sidak post hoc test was used. † Main effect of DS *vs*. DR (P<0.05), ‡ Main effect of exercise (P<0.05). *P<0.05, **P<0.01 ***P<0.001.

negatively associated with fat mass,[39] RMR and VO_2 were corrected for body mass using an analysis of covariance (ANCOVA). A trend persisted at BL for lower energy expenditure in DR women (P=0.11 for RMR and P=0.10 for VO_2), even when correcting for body mass. Moreover, the absolute rate of lipid utilisation was higher at BL in DS women with obesity compared to DR (Figure S1). These findings are further strengthened by recent studies on the spend-thrift *vs*. thrifty phenotypes,[8] and results from an independent cohort demonstrating that DR individuals with obesity have a greater adaptation in whole-body energy expenditure than DS after a 4-week hypocaloric diet.[40]

Variable	Baseline		Post-exercise training		Main effect *P*-value	
	Diet-sensitive	Diet-resistant	Diet-sensitive	Diet-resistant	Group	Time
n	10	10				
Age (years)	53.7 ± 7.3	53.2 ± 9.3	-	-		
Self-reported activity	1.55 ± 0.69	1.70 ± 0.68	-	-		
Height (cm)	165.85 ± 7.34	158.55 ± 4.99	-	-		
Body weight (kg)	110.67 ± 28.85	96.87 ± 17.55	111.07 ± 29.30	96.27 ±17.68	0.19	0.78
BMI (kg/m^2)	39.92 ± 8.00	38.66 ± 7.56	40.03 ± 8.20	38.38 ± 7.66	0.68	0.56
Waist circumference (cm)	123.6 ± 18.5	116.1±11.5	121.7±16.1	112.7±10.5[b]	0.28	<0.01
Body composition by DEXA						
Fat mass (kg)	53.5 ±19.0	50.5 ± 13.7	53.6 ± 19.3	49.6 ± 14.1[b]	0.64	0.13
Lean mass (kg)	52.9 ± 6.5	43.8 ± 4.1[a]	52.6 ± 6.5	44.2 ± 4.9[a]	<0.01	0.84
Body fat (%)	49.2 ± 5.4	53.0 ± 4.7[a]	49.3 ± 5.6	52.0 ± 5.2[a,b]	<0.05	0.09
Fasting blood biochemistry						
Fasting glucose (mmol/L)	5.2 ± 0.5	5.1 ± 0.6	5.5 ± 0.7	5.3 ± 0.6	0.53	0.14
HbA1c (%)	5.8 ± 0.4	5.6 ± 0.3	5.6 ± 0.4[b]	5.5 ± 0.3[b]	0.46	<0.001
Fasting insulin (pmol/L)	91.2 ± 50.4	61.4 ± 8.6	103.0 ± 58.3	60.4 ± 25.2[a]	<0.05	0.47
HOMA-IR	3.06 ± 1.78	2.00 ± 0.89	3.65 ± 2.40	2.08 ± 1.01[a]	0.11	0.31
Fasting triglycerides (mmol/L)	1.38 ± 0.49	1.54 ± 0.52	1.25 ± 0.42	1.35 ± 0.58	0.53	0.06
Total cholesterol (mmol/L)	5.30 ± 0.86	5.09 ± 0.89	5.33 ± 0.83	5.26 ± 0.93	0.71	0.34
HDL-cholesterol (mmol/L)	1.54 ± 0.26	1.47 ± 0.36	1.54 ± 0.094	1.50 ± 0.39	0.66	0.65
LDL cholesterol (mmol/L)	3.13 ± 0.77	2.95 ± 0.72	3.36 ± 0.74	3.22 ± 0.86	0.61	0.09
Creatine kinase (U/L)	127.8 ± 81.1	68.7 ± 22.0[a]	110.5 ± 37.3	72.9 ± 30.7[a]	<0.01	0.79
Metabolic and Fitness Testing						
Resting heart rate (BPM)	65 ± 9	69 ± 8	62 ± 10	69 ± 8	0.14	0.19
RMR (kcal/h)	91.7 ± 24.3	74.0 ± 10.9[a]	84.4 ± 13.7	76.7 ± 10.1	0.06	0.48
Resting VO_2 (mL/min)	308.5 ± 82.4	247.8 ± 35.7[a]	284.9 ± 47.2	255.4 ± 36.7	<0.05	0.47
Resting respiratory exchange ratio (RER)	0.80 ± 0.04	0.82 ± 0.07	0.78 ± 0.05	0.82 ± 0.04	0.17	0.63
Bench press (kg)	28.4 ± 4.0	23.9 ± 9.5	37.7 ± 6.5[b]	32.1 ± 9.5[b]	0.15	<0.001
Lateral pulldown (kg)	54.8 ± 7.8	44.4 ± 5.3[a]	61.9 ± 6.6[b]	49.1 ± 5.8[a,b]	<0.001	<0.001
Seated row (kg)	48.5 ± 9.4	41.3 ± 6.9[a]	65.2 ± 8.1[b]	50.2 ± 6.5[a,b]	<0.001	<0.001
Leg Press (kg)	80.3 ±17.2	62.5 ± 9.9[a]	106.6 ± 19.4[b]	83.4 ± 13.6[a,b]	<0.01	<0.001

***Table 1*: Exercise training selectively improves body composition in diet-resistant women with obesity.**
BMI, body mass index; HOMA-IR, homeostatic model assessment for insulin resistance; RMR, resting metabolic rate. Values are means±SD. Two-way ANOVA for repeated-measures with Holm-Sidak post hoc test.
[a] DS *vs.* DR ($P<0.05$).
[b] Effect of exercise ($P<0.05$).

The exercise intervention did not induce weight loss in either group, but exercise training decreased fat mass, waist circumference, and body fat (%) in DR women only (all exercise within DR $P<0.05$, two-way ANOVA for repeated-measures with Holm-Sidak post hoc test, Table 1, Figure 2b). Energy expenditure during an exercise bout, as assessed by a graded exercise test, did not differ between groups (Figure 2d and S1). However, heart rate was higher in DR women regardless of exercise training (main effect DS vs. DR $P<0.05$, two-way ANOVA for repeated-measures, Figure 2d). Furthermore, despite similar mass-specific cost of transport (amount of energy required to move 1 meter, Figure S1), the respiratory exchange ratio (RER), the absolute rate of substrate utilisation, and the relative contribution of these fuel sources to energy expenditure (%EE) indicated that DS women relied more on FA oxidation at higher work outputs compared DR women (main effect DS vs. DR $P<0.05$, two-way ANOVA for repeated-measures, Figure 2d and S1).

Measurements of muscle strength by isometric knee torque and predicted one-repetition maximum (1RM) revealed relative deficiencies in strength in DR women prior to the intervention (group within BL $P<0.01$, two-way ANOVA for repeated-measures with Holm-Sidak post hoc test, Figure 2e; Table 1). The combined aerobic and resistance exercise intervention improved muscle strength in both DR and DS groups (main effect exercise $P<0.001$, two-way ANOVA for repeated-measures, Figure 2e, Table 1). To determine if the improved muscle strength was due to muscle hypertrophy or changes in muscle fibre composition, we next examined muscle cross-sectional area (CSA) and muscle fibre type.

Consistent with our previous findings,[16] skeletal muscle from DR women at BL had significantly fewer type I fibres, with a trend for smaller CSA than DS women (P=0.06, two-way ANOVA for repeated-measures with Holm-Sidak post hoc test, Figure 2g and S1). Exercise training tended to increase % type I fibres in both groups (P=0.066, two-way ANOVA for repeated-measures with Holm-Sidak post hoc test, Figure 2g) but did not induce hypertrophy (Figure S1). Six weeks of exercise training is relatively short to observe changes in muscle CSA that result from increases in muscle protein synthesis. Thus, to determine if skeletal muscle hypertrophy was initiated, we quantified muscle protein concentration relative to muscle weight and observed that the exercise training increased muscle protein content in DR (exercise within DR P<0.001, two-way ANOVA for repeated-measures with Holm-Sidak post hoc test, Figure 2f).

Exercise training improves mitochondrial content and function in diet-resistant obesity

Obesity is associated with skeletal muscle mitochondrial dysfunction and remodelling which leads to lower mitochondrial content and impaired bioenergetic function.[41,42] In individuals with obesity, exercise stimulates skeletal muscle mitochondrial biogenesis and confers greater improvements in mitochondrial function compared to caloric restriction.[43] One of our primary aims was to determine the efficacy of exercise in improving skeletal muscle mitochondrial function in DR women. Markers of mitochondrial content, citrate synthase (CS) and succinate dehydrogenase activity, were lower in DR muscle compared to DS prior to exercise training (group within BL P<0.05, and main effect DS vs. DR P<0.05, two-way ANOVA for repeated-measures with Holm-Sidak post hoc test, Figure 3a; S2). Following the exercise intervention, CS activity increased in DR muscle (exercise within DR P<0.05, two-way ANOVA for repeated-measures with Holm-Sidak post hoc test). The exercise-induced increases in CS activity were not exclusively due to PGC1α-mediated mitochondrial biogenesis, as the exercise intervention increased muscle PGC1α expression in both DR and DS women (main effect of exercise P<0.05, two-way ANOVA for repeated-measures, Figure 3b).

Using high-resolution respirometry to assess mitochondrial function in biopsied *vastus lateralis* fibres, we next confirmed our previous findings of lower mitochondrial OXPHOS, oligomycin-induced leak respiration, and maximal respiration at BL in DR (group within BL P<0.05, two-way ANOVA for repeated-measures with Holm-Sidak post hoc test, Figure 3c). When normalising respiration to CS activity there were no differences at BL between groups (Figure S2), which suggests the differences in mitochondrial function at BL may partially be driven by mitochondrial content. Exercise training increased OXPHOS and maximal respiration in DR but not DS individuals (exercise within DR P<0.05, two-way ANOVA for repeated-measures with Holm-Sidak post hoc test, Figure 3c). These exercise-induced improvements of mitochondrial function in DR muscle were cell autonomous, as these results were recapitulated in primary myotubes isolated from participants. Cultured myotubes from DR women exhibited increased basal, ATP-coupled, and maximal oxygen consumption following exercise training (all exercise within DR P<0.01, two-way ANOVA for repeated-measures with Holm-Sidak post hoc test, Figure 3d; S2). Moreover, exercise training resulted in a more fused mitochondrial reticulum in DR myotubes, as indicated by an increase in mitochondrial length (exercise within DR P<0.05, two-way ANOVA for repeated-measures with Holm-Sidak post hoc test, Figure 3e). Fluorometric-based analysis of H_2O_2 emission was conducted simultaneously with respiratory measurements in biopsied myofibers and revealed no differences between DS and DR per mg muscle (Figure S2). However, H_2O_2 emissions were ~38% higher in DR muscle during oligomycin-induced proton leak at BL, which was attenuated after exercise training (group within BL P<0.05, exercise within DR P<0.05, two-way ANOVA for repeated-measures with Holm-Sidak post hoc test, Figure 3f).

Skeletal muscle mitochondrial proton leak contributes significantly to metabolic rate and is achieved through mitochondrial inner membrane carrier proteins including uncoupling protein-3 (UCP3) and adenine nucleotide translocator (ANT).[44–47] We previously reported lower mitochondrial proton leak in muscle from DR women across three separate study cohorts.[11,12,17] We detected lower muscle *UCP3* gene expression in DR women,[11] but failed to detect differences in UCP3 protein expression in primary myotubes derived from DR and DS women.[12] Here, we did not observe differences in UCP3 protein expression between groups, but the relative protein expression of adenine nucleotide translocase (ANT) was lower in DR muscle independent of exercise training (main effect DS vs. DR P<0.05, two-way ANOVA for repeated-measures, Figure 3g). ANT accounts for approximately 50% of basal proton leak in muscle,[47] suggesting that differences in proton leak between DS and DR individuals may be attributable to differential expression and activity of ANT.

The mitochondrial electron transport chain (ETC) complexes I, III, and IV can form higher-order supercomplexes (SCs) to facilitate efficient energy transduction and decrease ROS production.[48] We sought to determine if the improvements in mitochondrial function in DR muscle were attributable to reorganisation and enhanced formation of ETC SCs that can occur with exercise training.[49] Muscle from DR women contained lower amounts of CIII and CIV containing SCs,

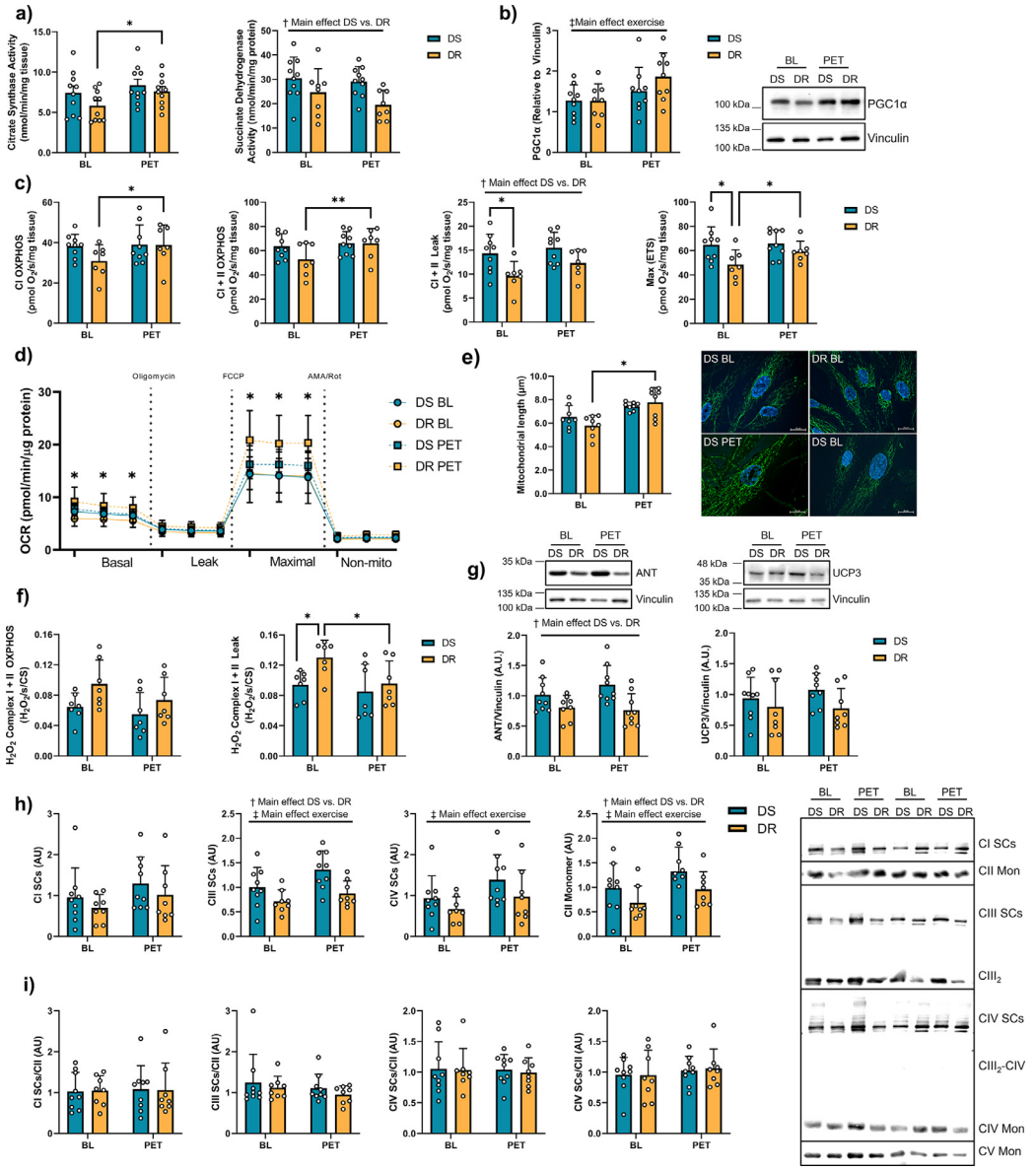

Figure 3. Exercise training preferentially improves mitochondrial content and function in diet-resistant women with obesity. (a) Citrate synthase activity (CS) tended to be lower in *vastus lateralis* from DR women compared to DS at BL (P=0.066). CS activity increased in DR muscle only at PET. Succinate dehydrogenase activity was lower in DR muscle regardless of exercise training, (n=10). **(b)** PGC1α protein expression increased in both DS and DR muscle following exercise training, (n=9 DS, n=8 DR). **(c)** High-resolution respiratory flux per mg of saponin-permeabilised *vastus lateralis* muscle. Exercise training enhanced complex I (CI) oxidative phosphorylation (OXPHOS) and CI+II OXPHOS, and improved FCCP-induced maximal respiration in DR muscle. However, oligomycin-induced leak respiration was lower in DR muscle, regardless of exercise training. (n=9 DS, n=7 DR). **(d)** Seahorse analysis on biopsy-derived primary myotubes demonstrated that basal and maximal oxygen consumption was enhanced with exercise training in DR women, (n=9). **(e)** Mitochondrial length increased with exercise training in primary myoblasts isolated from DR women. Representative images are shown beside the graph; scale bars, 20 µm, (n=8). **(f)** Fluorometric quantification of H_2O_2 emission demonstrated that oligomycin-induced H_2O_2 was higher at BL in DR *vastus lateralis* when corrected for mitochondrial content using citrate synthase (CS) activity. Exercise training decreased H_2O_2 emission in DR muscle, (n=7). **(g)** Immunoblot analyses revealed protein expression of the adenine nucleotide translocase was lower in DR *vastus lateralis* compared to DS regardless of exercise training. In contrast, protein expression of UCP3 did not differ, (n=9 DS, n=8 DR). **(h)** Skeletal muscle biopsies were solubilized with 1.5% vol/wt digitonin prior to separation via BN-PAGE. *Vastus lateralis* from DR women had lower expression of CIII-containing SC and CII monomer regardless of exercise training. Exercise training enhanced CIII and CIV supercomplex formation, as well as CII and CV monomer expression in both groups. **(i)** When normalising SCs to CII, no differences were observed in CIII or CIV supercomplex formation (n=9 DS, n=8 DR). All values are presented as means ± SD. A two-way ANOVA for repeated-measures with Holm-Sidak post hoc test was used. † Main effect of DS *vs*. DR (P<0.05), ‡ Main effect of exercise (P<0.05). *P<0.05, **P<0.01 ***P<0.001.

but not CI SCs (main effect of DS vs. DR $P<0.01$ for CIII and $P<0.05$ CIV, two-way ANOVA for repeated-measures, Figure 3h). CII levels also trended lower in DR muscle at BL ($P=0.062$, two-way ANOVA for repeated-measures with Holm-Sidak post hoc test). Exercise training increased muscle CIII and CIV SCs and CII levels in both DR and DS women (main effect of exercise $P<0.05$, two-way ANOVA for repeated measures), with a trend for increased CI SCs (main effect exercise $P=0.068$, two-way ANOVA for repeated measures). Consistent with the observation of lower mitochondrial content in DR individuals, these effects disappear when SC levels were expressed relative to CII (Figure 3i). These results were similar in patient-derived primary myotubes, as DR myotubes had lower CI, CIII, and CIV SCs at BL (group within BL $P<0.05$ for all, two-way ANOVA for repeated-measures with Holm-Sidak post hoc test, Figure S3). However, when SCs were normalised to CII, exercise training increased CIV SCs in DR primary myotubes only (exercise within DR $P<0.05$ two-way ANOVA for repeated-measures with Holm-Sidak post hoc test, Figure S3).

Exercise training alters the DR metabolite network

A few studies have assessed metabolic signatures in plasma/serum from obese individuals following weight loss,[50–53] with the hypothesis that baseline energy metabolites in plasma are reflective of whole-body metabolism, and indicate capacity for weight loss. We propose that the muscle metabolome may be more reflective of whole-body energy metabolism as muscle is an important contributor to metabolism. Here, we used rigorous liquid chromatography mass spectroscopy (LCMS) approaches paired with bioinformatics and machine learning analyses to determine differences in the muscle metabolism between DR and DS women at BL and after exercise training.

We first quantified 89 metabolites in skeletal muscle using ion-pairing LCMS. Consistent with previous attempts in identifying plasma biomarkers that predict weight loss susceptibility,[51] we failed to detect statistically significant differences at baseline in discrete metabolites between DS and DR muscle (Figure 4a). Of note, L-γ-glutamyl-L-cysteine was lower in DR muscle at BL ($P<0.05$, two-tailed Student's t-test); however, this failed to achieve significance after FDR correction. L-γ-glutamyl-L-cysteine is the immediate precursor to glutathione (GSH), and we have consistently detected impaired GSH redox in separate cohorts of DR individuals.[12,17] Following the exercise intervention, serine was significantly higher in DR muscle compared to DS (group within PET $P<0.01$, two-way ANOVA for repeated-measures with Holm-Sidak post hoc test, Figure 4a and 4b). Serine is a non-essential amino acid that acts as a central metabolic node in 1-carbon metabolism (1C) that links folate and methionine cycles to support the synthesis of sphingolipids, phospholipids, purines, and GSH redox.[54,55]

We coupled muscle metabolomics analyses with MS/MS analysis of plasma amino acids to determine if the alterations in muscle serine concentrations were reflected in circulation. Similar to the muscle metabolome, we failed to detect differences in single circulating analytes at BL; however, sarcosine was higher in DR individuals following exercise training (group within PET $P<0.001$, two-way ANOVA for repeated-measures with Holm-Sidak post hoc test, Figure 4c). Sarcosine is closely linked to serine through mitochondrial 1C reactions.[54]

We next employed the machine learning feature selection method, ReliefF, to identify metabolites in muscle and plasma that are most relevant for differentiating between the cohorts of DR and DS women at BL and following the exercise intervention. The individual metabolites with a high discrepancy between DR and DS plasma and muscle were serine and branched-chain amino acids (BCAAs), which suggests that pathways involving these metabolites are instrumental in driving the differing metabolic phenotypes (Figure 4b muscle; 4c plasma).

To further dissect the differences in metabolism between DS and DR women, we subsequently compared the distance correlations between metabolites (Figure S5-S7).[31] Metabolite distance correlation networks can identify the key metabolic pathways that are dysregulated between distinct disease phenotypes, even before changes in discrete metabolites occur.[56] At BL, ADP was ranked as the largest functional difference in the muscle correlation network (Figure 4d). However, it is the ratio of ATP, ADP, and AMP pools that reflect cellular energy status and is crucial in controlling anabolic and catabolic metabolic pathways; Thus, we analysed the correlation network between energy charge [(ATP +0.5*ADP)/(ATP+ADP+AMP)][57] and muscle metabolites (Figure 4f). At BL, the pathways with enriched metabolites correlating with energy charge exclusive to DS muscle were BCAA catabolism, butyrate metabolism, and O-phosphorylethanolamine (PE) biosynthesis (Figure 4f). In contrast, enriched metabolites correlating to energy charge exclusive to DR were histidine and pyruvate metabolism. After exercise training, correlation analyses indicated a shift in the pathways driving energy metabolism in DR muscle towards the profile exhibited by DS muscle, with enriched metabolite sets centering around the citric acid cycle, and amino acid and propanoate metabolism in both DR and DS muscle. Moreover, the biosynthesis of cardiolipin, a strong biomarker for mitochondrial content,[58] and metabolites involved in the mitochondrial electron transport chain were exclusively enriched in DR muscle after exercise training, which supports the exercise-induced increase in mitochondrial content in DR muscle. Taken together, the shift in the metabolome profile in DR muscle suggests that exercise training preferentially enhances oxidative capacity in DR women (Figure 4g).

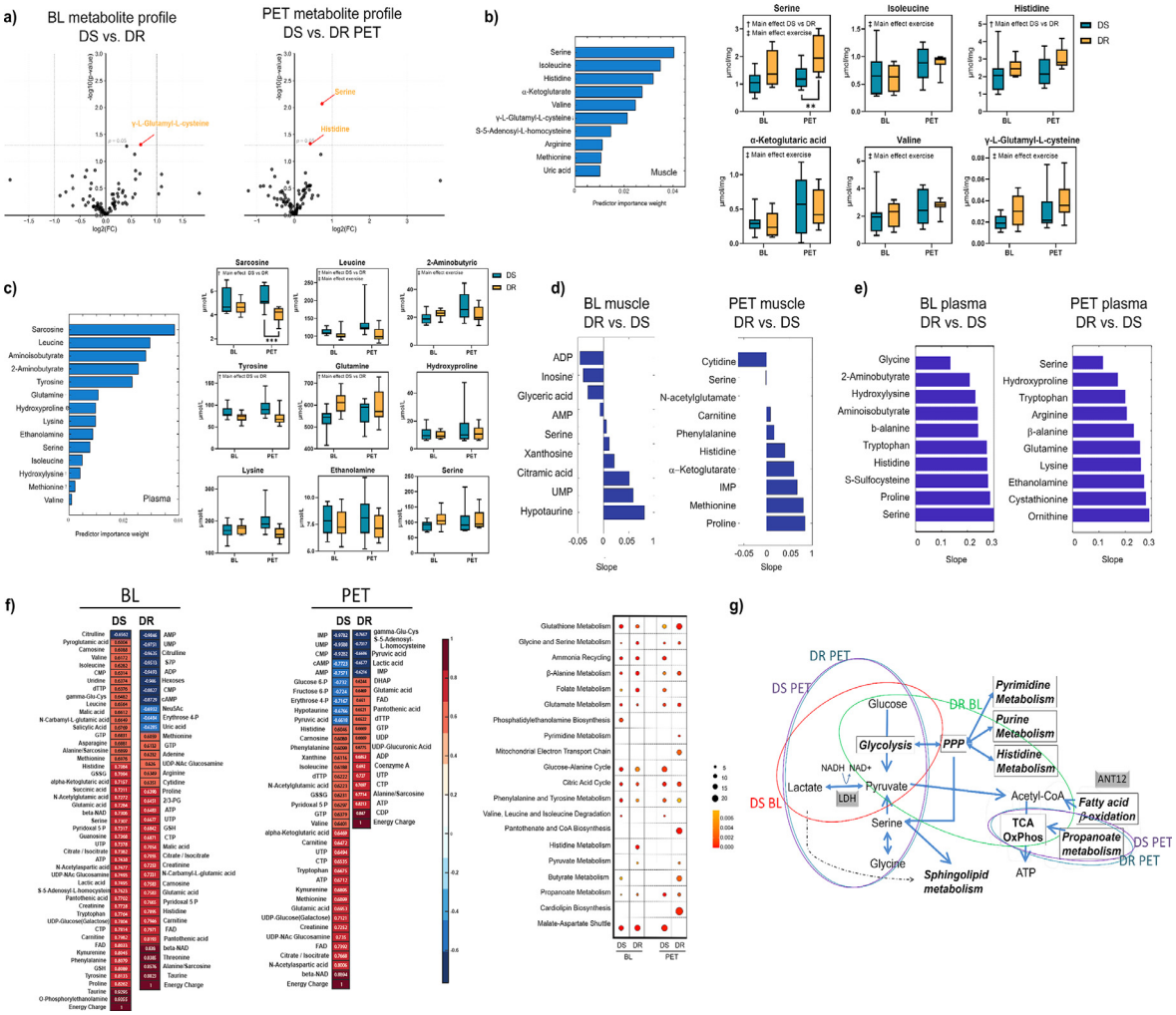

Figure 4. Exercise training improves the skeletal muscle metabolite network in diet-resistant women with obesity. (a-f) Metabolomic analyses of *vastus lateralis* and plasma samples from DR and DS women with obesity at BL and PET. **(a)** Volcano plots of metabolite profiles from *vastus lateralis* at BL and PET. Significant features ($P<0.05$, Student's t-test) highlighted. Serine was higher in DR muscle following exercise training (with FDR correction), (n=9 DS, n=8 DR). **(b)** Selection of the most significantly different features between DR and DS at BL and PET from metabolomics measurements in *vastus lateralis*. Shown are all features with ReliefF weight measure over 0 (significant contributors to a classification model), (n=9 DS, n=8 DR). **(c)** Selection of the most significantly different features between DR and DS plasma at BL and PET. Shown are all features with ReliefF weight measure over 0 (significant contributors to a classification model). Sarcosine was lower in DR plasma after exercise training. *$P<0.05$ with FDR correction, (n=10). **(d)** Selection of metabolites with the largest change in their distance correlation network in skeletal muscle (n=9 DS, n=8 DR). See also Figure S5 and S6. **(e)** Selection of metabolites with the largest change in their distance correlation network in plasma (n=9 DS, n=8 DR). See also Figure S5 and S7. **(f)** Selection of skeletal muscle metabolites with the largest change in their distance correlation network with adenylate energy charge [(ATP+0.5*ADP)/(ATP+ADP+AMP)], with pathway enrichment analysis based on these metabolites. Shown are metabolite partners with distance correlation > 0.7; $P<0.02$, (n=9 DS, n=8 DR). **(g)** Proposed pathway differences in skeletal muscle energy metabolism related to the adenylate correlation network.

Serine metabolism is differentially regulated between diet-resistant and diet-sensitive obesity following exercise training

The machine learning analyses identified serine as a significant feature in both plasma and muscle metabolites. Metabolite distance correlation networks in plasma suggest that the route for serine production and/or utilisation differed significantly between DS and DR women, despite similar concentrations in plasma (Figures 4e, 5a). Serine is involved in the first step of *de novo* sphingolipid synthesis, in which serine palmitoyltransferase (SPT) catalyses the major-controlling reaction involving the condensation of serine and palmitoyl-CoA.[59] The accumulation of sphingolipids in skeletal

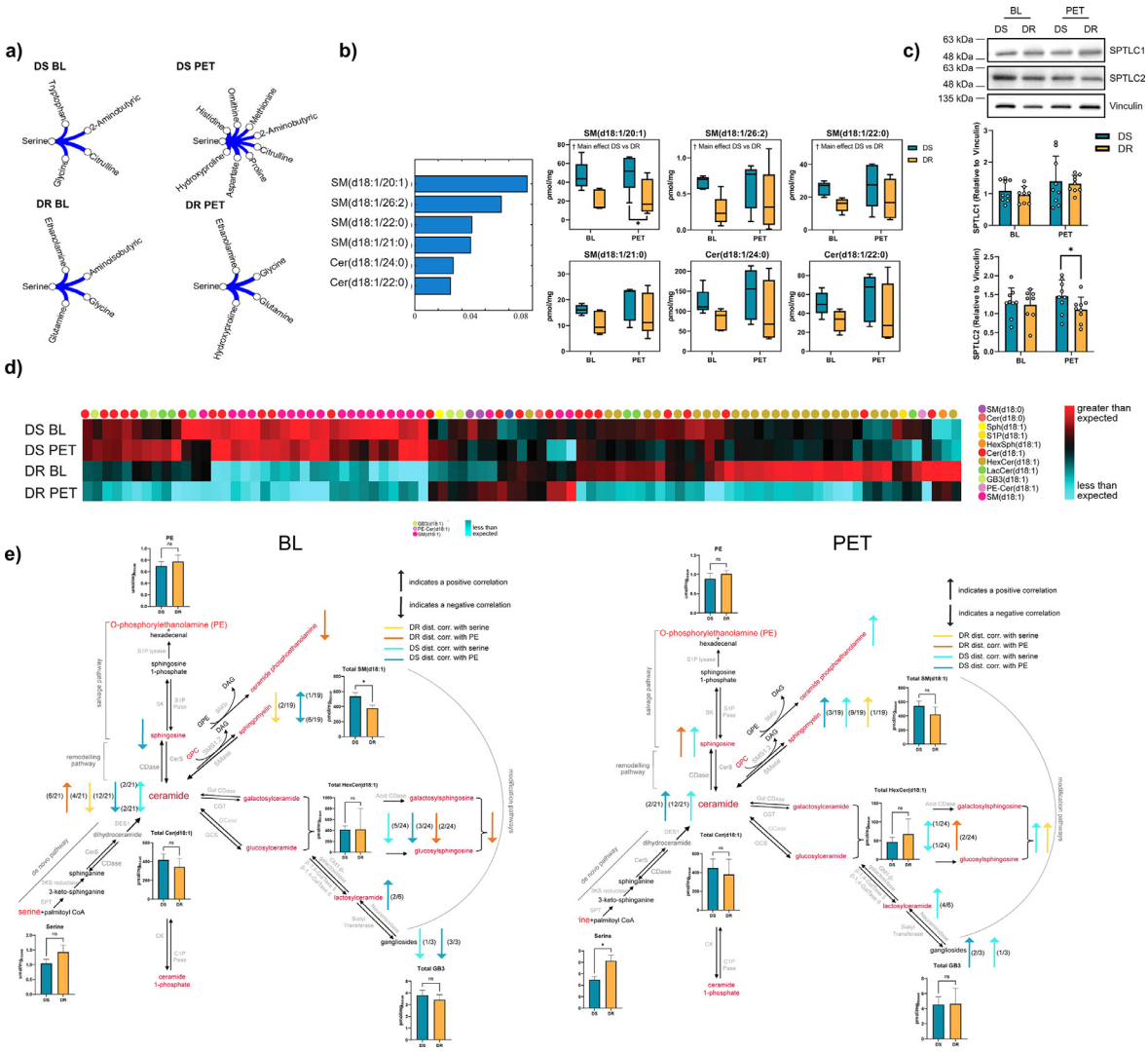

Figure 5. Exercise training differentially alters the serine-sphingolipid muscle metabolite networks in diet-sensitive and diet-resistant women with obesity. (a-e) Enriched metabolite networks reveal differing profiles in *vastus lateralis* from DR and DS individuals at BL and PET. **(a)** The correlation network for plasma serine. Shown are partners with distance correlation > 0.7; $P<0.02$, (n=10). **(b)** Selection of the most significantly different sphingolipid features in *vastus lateralis*. Shown are features with ReliefF weight measure over 0.03 (major contributors to a classification model), (*n*=5). **(C)** Immunoblot analyses revealed relative protein expression of SPTLC1 did not differ between DR and DS, whereas expression of SPTLC2 was lower in DR skeletal muscle following exercise training. (**P*<0.05, Two-way ANOVA for repeated-measures with Holm-Sidak post hoc test, *n*=9). **(d)** Heatmap clustering of relative sphingolipid level changes compared to the total sample mean in the DS and DR groups before and after exercise. Data were log-transformed and z-scored. **(e)** Sphingolipid metabolic pathway indicating network correlations are distinct in DR and DS groups at baseline. Direction of arrows indicates direction of correlation; arrow colours indicate correlations between sphingolipid species at the beginning (serine) or end (O-phosphorylethanolamine (PE)) of the sphingolipid metabolic pathway in either the DR or DS groups. The number of species with significant correlations in each subclass (absolute correlation level over 0.6 with $P<0.05$) are indicated. Data in bar graphs represent mean ± SEM. (**P*< 0.05, t−test with Welch's correction, *n*=5). See also Figure S4.

muscle has been implicated in the development of insulin resistance by interfering with insulin-stimulated glucose uptake,[60,61] which could contribute to the emerging metabolic phenotype in DS women. Thus, we analysed the sphingolipid profile of *vastus lateralis* from a subset of samples to determine if there were differences in sphingolipid metabolism. Since limited sample availability rendered us unable to include age-, weight-, and BMI-paired sets of DR and DS samples, we concentrated on distance correlations of sphingolipids and serine to identify differences in sphingolipid metabolism between groups. Distinct d18:1 species of

sphingomyelins (SM) were higher in DS *vastus lateralis* when collapsing across timepoints, with ReliefF analyses also identifying this set of sphingomyelins as the most significant features for classification between groups (main effect DS vs. DR $P<0.05$, two-way ANOVA for repeated-measures with Holm-Sidak post hoc test, Figure 5b). Heatmap clustering of log-transformed and z-scored lipid levels showed clustering of the majority of SM species, with SM abundance greater in DS muscle compared to DR, regardless of exercise (Figure 5d). SM levels have been shown to be higher in obese patients with type 2 diabetes and to inversely correlate with insulin resistance in mice.[60,62,63] Exercise training lowered all detected hexosyl-ceramide species in DR muscle, whereas there was no change in relative lipid levels in the DS muscle following the exercise intervention.

To further explore differences in the sphingolipid metabolic network between the DR and DS *vastus lateralis*, we calculated the correlation network for all measured sphingolipids with serine, involved in the first step of sphingolipid synthesis, and PE, the catabolic exit point of sphingolipids. Serine was positively associated with several species of ceramides and sphingomyelins both at BL and PET in DS muscle, and only at BL in DR muscle (Figure 5e and S4). Immunoblot analysis revealed that DS muscle had augmented protein expression of the SPTLC2 subunit of SPT following exercise training, but not the SPTLC1 subunit (group within PET $P<0.05$, two-way ANOVA for repeated-measures with Holm-Sidak post hoc test, Figure 5c), supportive of increased sphingolipid synthesis. Furthermore, PE negatively correlated with nearly every sphingolipid subclass except PE-Cer and lactosylceramides in DS muscle (both BL and PET), suggesting degradation via the modification pathway (Figure 5e and S4). In contrast, nearly all sphingolipid correlations with both serine and PE disappeared at the presented level of significance in DR *vastus lateralis* after exercise training. Of note, there was a negative correlation between PE and ceramide phosphoethanolamine PE-Cer(d18:1/24:0) in DR muscle at BL, suggesting that in the DR group *de novo* synthesised ceramides are preferentially shunted towards PE-Cer rather than SM.

Discussion

Despite extensive knowledge of the overarching causes and consequences of obesity, individual weight loss success in response to caloric restriction, medication and surgery is extremely variable [reviewed in Dent et al. 2020[4]]. Here, we provide evidence that capacity for rapid diet-induced weight loss in women with obesity is associated with central adiposity and increased risk of metabolic syndrome prior to weight loss. Furthermore, we demonstrate that women with a documented history of minimal diet-induced weight loss accrue greater benefits from exercise training compared to women who lose weight rapidly from caloric restriction. Our integrated analysis of the *m. vastus lateralis* metabolome and sphingolipidome identified distinct differences in metabolism that further distinguished the DR and DS phenotypes, and corroborate the differential responses to exercise training. Taken together, these findings have significant implications for the development of more effective and personalised treatment strategies for obesity.

BMI is a widely used, but flawed method to assess and classify the extent of obesity. However, it is well accepted that BMI *per se* is a poor predictor of individual risk for cardiometabolic diseases. A recent meta-analysis of 72 cohorts consisting of over 2 million participants demonstrated that central adiposity is positively associated with a higher risk of all-cause mortality, independent of overall adiposity.[64] It should be acknowledged that the cohorts of women recruited for the DEXA scans and the exercise intervention were on average 7 years older and had a BMI of 4.9 kg/m^2 (12%) lower than the overall population of women in the OHWMP. Mechanistic studies have demonstrated that visceral adipocytes express greater levels of hormone-sensitive lipase and are more resistant to the anti-lipolytic effects of insulin.[65,66] The increased sensitivity to lipolytic stimuli[67,68] contributes to hypertriglyceridemia due to the release of fatty acids into circulation in close proximity to the portal vein.[65,69] Consistent with our findings, our machine learning network-based feature selection approaches of the skeletal muscle metabolome and sphingolipidome suggest that DS ceramide synthesis and utilisation are enhanced in DS muscle as indicated by the serine/PE correlation networks, which supports a greater risk of metabolic syndrome in DS individuals.[60,70] Therefore, despite the weight loss benefits of a diet-sensitive phenotype, these individuals are at a greater risk for the metabolic complications of obesity.

Studies assessing the efficacy of exercise as a therapeutic treatment to induce weight loss have produced inconsistent results and collectively have contributed to the generally diet-focused approaches to treat obesity. While it is established that exercise in combination with caloric restriction elicits both greater initial, and sustained weight loss,[71–73] the idiom "you cannot outrun a bad diet" is based on a decade of research demonstrating that decreased energy intake generally leads to greater weight loss than increased energy expenditure through exercise.[73–75] In theory, energy expenditure must exceed energy intake to induce successful weight loss. Attempts to explain inadequate weight loss in response to exercise interventions have focused on the low doses of prescribed exercise, heterogeneity in exercise response,[76] and the commonly observed compensatory increase in caloric intake.[77] However, in cases in which diet-adherent individuals fail to achieve successful weight loss through caloric restriction, exercise may

preferentially enhance their weight loss capacity by reprogramming skeletal muscle metabolism to enhance oxidative processes, consistent with our findings in biopsied muscle and derived primary muscle cells.

Our findings of a higher body fat (%) and lower lean mass in DR individuals support the use of exercise to enhance weight loss capacity in diet-resistant obesity, as exercise-induced weight loss significantly decreases total fat mass to a greater extent than diet-induced weight loss.[78] Exercise when combined with caloric restriction attenuates the loss of muscle mass, improves myofiber composition, and stimulates muscle protein synthesis in individuals with obesity.[79,80] Type II fibres, which are more abundant in DR muscle, adapt first to exercise training by recruiting satellite cells for regeneration.[81] Moreover, gene set enrichment analysis in *rectus femoris* muscle previously demonstrated decreased expression of ribosomal proteins from DR individuals with obesity as compared to DS,[16] for which resistance exercise has been shown to induce ribosomal biogenesis.[82] While the relatively small sample size is a limitation of our study and a longer training intervention would be required to observe myofiber hypertrophy, our findings demonstrate that exercise may be a clinically important intervention in individuals with diet-resistant obesity. Of note, occasionally limited sample availability rendered us unable to perform all molecular analyses on skeletal muscle from all participants, and we were unable to conduct multivariate analysis to adjust for baseline characteristics due to the low sample size.

While rapid weight loss and improvements in insulin sensitivity are observed with diet-induced weight loss, energy restriction does not induce mitochondrial biogenesis or improve mitochondrial function.[43] In contrast, exercise elicits rapid improvements in mitochondrial bioenergetic function and content in as little as 5 days.[43,83] Here, we demonstrate that the impaired skeletal muscle mitochondrial function that we have consistently observed in the diet-resistant phenotype is partly attributable to lower mitochondrial content, which is preferentially enhanced in DR muscle with exercise training. The exercise-induced increases in oxidative capacity and ETC supercomplexes, as measured in both skeletal muscle and biopsy-derived primary myotubes, further suggest that exercise reprograms satellite cells in diet-resistant obesity through epigenetic mechanisms, as even a single bout of exercise decreases the methylation of promotors for *PPARGC1A, PDK4* and *PPARD* and increases the expression of these genes.[84]

In summary, exercise training improves body composition and skeletal muscle bioenergetic function in individuals with obesity who do not respond adequately to energy restriction. In addition, although the diet-sensitive phenotype would appear inherently preferable to a diet-resistant state, the same metabolic characteristics that enable rapid lipolysis and loss of visceral adipose tissue make DS individuals more susceptible to metabolic diseases prior to weight loss. Altogether, our findings are supportive of current guidelines for exercise and cardiometabolic health, and demonstrate preferential improvements in metabolism for diet-resistant obesity with exercise training.

Contributors

Conceptualisation and methodology:CAP, DPB, IA, MDF, SALB, ED, FH, MCC, RM, RD, MEH. Data curation:CAP, DPB, BGH, GP, IA, DAP, AC, COD, ABT. Formal analysis: CAP, DPB, BGH, GP, IA, DAP, SALB, MCC. Funding acquisition: RM, MEH, SALB, MDF. Writing original draft: CAP, DPB, GP, IA, MCC, MEH. Writing-review & editing: CAP, DPB, BGH, GP, IA, DAP, AC, COD, ABT, MDF, SALB, ED, FH, RM, RD, MEH. Directly accessed and verified the underlying data: CAP, DPB, BGH, GP, IA, DAP, SALB, MCC, RD, MEH. All authors have read and approved the manuscript.

Data sharing statement

The metabolomic and lipidomic data sets have been deposited in the NRC Digital Repository from the National Research Council Canada, with the Record Identified 908ee158-bc61-461c-9e56-79542733fdd2. Clinical data used for analysis in this study are held at the Ottawa Hospital and the University of Ottawa. Requests for data may be shared with the use of an institutional data sharing agreement. Further information and requests for reagents and resources should be directed toward the corresponding author, Mary-Ellen Harper (mharper@uottawa.ca).

Declaration of interests

The authors declare no conflicts of interest.

Acknowledgements

The authors would like to thank all the participants. This research was supported by the Canadian Institutes of Health Research (CIHR-INMD and FDN-143278, MEH; CAN-163902, SALB; CIHR PJT-148634, MDF). The authors would like to thank the following individuals and groups for their excellent support: Heather Doelle, Evan Bushnik, James Ryan, James F. Markworth, Majid Nikpay, Keili Shepherd, Kelli E. King, Shannon Thompson, Kevin Semeniuk, Luzia Hintze, Nina Hadzimustafic, and the Louise Pelletier Histology Core facility (RRID: SCR_021737).

Supplementary materials

Supplementary material associated with this article can be found in the online version at doi:10.1016/j.ebiom.2022.104192.

References

1 Flegal KM, Kit BK, Orpana H, Graubard BI. Association of all-cause mortality with overweight and obesity using standard body mass index categories: a systematic review and meta-analysis. *JAMA*. 2013;309(1):71–82.
2 Heymsfield SB, Wadden TA. Mechanisms, pathophysiology, and management of obesity. *N Engl J Med*. 2017;376(3):254–266.
3 Lemstra M, Bird Y, Nwankwo C, Rogers M, Moraros J. Weight loss intervention adherence and factors promoting adherence: a meta-analysis. *Patient Prefer Adher*. 2016;10:1547–1559.
4 Dent R, McPherson R, Harper M-E. Factors affecting weight loss variability in obesity. *Metabolism*. 2020;113:154388.
5 Stinson EJ, Piaggi P, Votruba SB, et al. Is dietary nonadherence unique to obesity and weight loss? Results from a randomized clinical trial. *Obesity (Silver Spring)*. 2020;28(11):2020–2027.
6 Leibel RL, Rosenbaum M, Hirsch J. Changes in energy expenditure resulting from altered body weight. *N Engl J Med*. 1995;332(10):621–628.
7 Rosenbaum M, Leibel RL. Adaptive thermogenesis in humans. *Int J Obes*. 2010;34(1):S47–S55.
8 Reinhardt M, Thearle MS, Ibrahim M, et al. A human thrifty phenotype associated with less weight loss during caloric restriction. *Diabetes*. 2015;64(8):2859–2867.
9 Tremblay A, Royer MM, Chaput JP, Doucet E. Adaptive thermogenesis can make a difference in the ability of obese individuals to lose body weight. *Int J Obes*. 2013;37(6):759–764.
10 Vinales KL, Begaye B, Bogardus C, Walter M, Krakoff J, Piaggi P. FGF21 is a hormonal mediator of the human "thrifty" metabolic phenotype. *Diabetes*. 2019;68(2):318–323.
11 Harper ME, Dent R, Monemdjou S, et al. Decreased mitochondrial proton leak and reduced expression of uncoupling protein 3 in skeletal muscle of obese diet-resistant women. *Diabetes*. 2002;51(8):2459–2466.
12 Thrush AB, Zhang R, Chen W, et al. Lower mitochondrial proton leak and decreased glutathione redox in primary muscle cells of obese diet-resistant versus diet-sensitive humans. *J Clin Endocrinol Metab*. 2014;99(11):4223–4230.
13 Adamo KB, Dent R, Langefeld CD, et al. Peroxisome proliferator-activated receptor γ 2 and acyl-CoA synthetase 5 polymorphisms influence diet response. *Obesity (Silver Spring)*. 2007;15(5):1068–1075.
14 Matsuo T, Nakata Y, Katayama Y, et al. PPARG genotype accounts for part of individual variation in body weight reduction in response to calorie restriction. *Obesity (Silver Spring)*. 2009;17(10):1924–1931.
15 Nikpay M, Lau P, Soubeyrand S, et al. SGCG rs679482 associates with weight loss success in response to an intensively supervised outpatient program. *Diabetes*. 2020;69(9):2017–2026.
16 Gerrits MF, Ghosh S, Kavaslar N, et al. Distinct skeletal muscle fiber characteristics and gene expression in diet-sensitive versus diet-resistant obesity. *J Lipid Res*. 2010;51(8):2394–2404.
17 Thrush AB, Antoun G, Nikpay M, et al. Diet-resistant obesity is characterized by a distinct plasma proteomic signature and impaired muscle fiber metabolism. *Int J Obes*. 2018;42(3):353–362.
18 Dent RM, Penwarden RM, Harris N, Hotz SB. Development and evaluation of patient-centered software for a weight-management clinic. *Obes Res*. 2002;10(7):651–656.
19 Brzycki M. *A Practical Approach to Strength Training*. Grand Rapids (MI): Masters Press; 1989.
20 Haman F, Péronnet F, Kenny GP, et al. Effect of cold exposure on fuel utilization in humans: plasma glucose, muscle glycogen, and lipids. *J Appl Physiol*. 2002;93(1):77–84.
21 Borg GA V. Psychophysical bases of perceived exertion. *Med Sci Sport Exerc*. 1982;14(5):377–381.
22 Bloemberg D, Quadrilatero J. Rapid determination of myosin heavy chain expression in rat, mouse, and human skeletal muscle using multicolor immunofluorescence analysis. *PLoS One*. 2012;7(4):e35273.
23 Mookerjee SA, Gerencser AA, Nicholls DG, Brand MD. Quantifying intracellular rates of glycolytic and oxidative ATP production and consumption using extracellular flux measurements. *J Biol Chem*. 2017;292(17):7189–7207.
24 Pileggi CA, Hedges CP, Segovia SA, et al. Maternal high fat diet alters skeletal muscle mitochondrial catalytic activity in adult male rat offspring. *Front Physiol*. 2016;7:546.
25 Acín-Pérez R, Fernández-Silva P, Peleato ML, Pérez-Martos A, Enriquez JA. Respiratory active mitochondrial supercomplexes. *Mol Cell*. 2008;32(4):529–539.
26 Lu W, Clasquin MF, Melamud E, Amador-Noguez D, Caudy AA, Rabinowitz JD. Metabolomic analysis via reversed-phase ion-pairing liquid chromatography coupled to a stand alone orbitrap mass spectrometer. *Anal Chem*. 2010;82(8):3212–3221.
27 Waterval WAH, Scheijen JLJM, Ortmans-Ploemen MMJC, Habets-van der Poel CD, Bierau J. Quantitative UPLC-MS/MS analysis of underivatised amino acids in body fluids is a reliable tool for the diagnosis and follow-up of patients with inborn errors of metabolism. *Clin Chim Acta*. 2009;407(1–2):36–42.
28 Bligh EG, Dyer WJ. A rapid method of total lipid extraction and purification. *Can J Biochem Physiol*. 1959;37(8):911–917.
29 Granger MW, Liu H, Fowler CF, et al. Distinct disruptions in Land's cycle remodeling of glycerophosphocholines in murine cortex mark symptomatic onset and progression in two Alzheimer's disease mouse models. *J Neurochem*. 2019;149(4):499–517.
30 Robnik-Šikonja M, Kononenko I. Theoretical and empirical analysis of ReliefF and RReliefF. *Mach Learn*. 2003;53(1):23–69.
31 Székely GJ, Rizzo ML, Bakirov NK. Measuring and testing dependence by correlation of distances. *Ann Stat*. 2007;35(6):2769–2794.
32 Pouliot M-C, Després J-P, Lemieux S, et al. Waist circumference and abdominal sagittal diameter: best simple anthropometric indexes of abdominal visceral adipose tissue accumulation and related cardiovascular risk in men and women. *Am J Cardiol*. 1994;73(7):460–468.
33 Chaston TB, Dixon JB. Factors associated with percent change in visceral versus subcutaneous abdominal fat during weight loss: findings from a systematic review. *Int J Obes*. 2008;32(4):619–628.
34 Knudsen N, Laurberg P, Rasmussen LB, et al. Small differences in thyroid function may be important for body mass index and the occurrence of obesity in the population. *J Clin Endocrinol Metab*. 2005;90(7):4019–4024.
35 Expert Panel on Detection E. Executive summary of the third report of the National Cholesterol Education Program (NCEP) expert panel on detection, evaluation, and treatment of high blood cholesterol in adults (adult treatment panel III). *JAMA*. 2001;285(19):2486–2497.
36 Dehghan M, Merchant AT. Is bioelectrical impedance accurate for use in large epidemiological studies? *Nutr J*. 2008;7(1):1–7.
37 Lavie CJ, Ozemek C, Carbone S, Katzmarzyk PT, Blair SN. Sedentary behavior, exercise, and cardiovascular health. *Circ Res*. 2019;124(5):799–815.
38 Barry VW, Caputo JL, Kang M. The joint association of fitness and fatness on cardiovascular disease mortality: a meta-analysis. *Prog Cardiovasc Dis*. 2018;61(2):136–141.
39 Halliday D, Hesp R, Stalley SF, Warwick PM, Altman DG, Garrow JS. Resting metabolic rate, weight, surface area and body composition in obese women. *Int J Obes*. 1979;3(1):1–6.
40 Whytock KL, Corbin KD, Parsons SA, et al. Metabolic adaptation characterizes short-term resistance to weight loss induced by a low-calorie diet in overweight/obese individuals. *Am J Clin Nutr*. 2021;114(1):267–280.
41 Pileggi CA, Parmar G, Harper M. The lifecycle of skeletal muscle mitochondria in obesity. *Obes Rev*. 2021;22(5):e13164.
42 Ritov VB, Menshikova EV, He J, Ferrell RE, Goodpaster BH, Kelley DE. Deficiency of subsarcolemmal mitochondria in obesity and type 2 diabetes. *Diabetes*. 2005;54(1):8–14.
43 Menshikova EV, Ritov VB, Dube JJ, et al. Calorie restriction-induced weight loss and exercise have differential effects on skeletal muscle mitochondria despite similar effects on insulin sensitivity. *J Gerontol A Biol Sci Med Sci*. 2017;73(1):81–87.
44 Rolfe DF, Brand MD. Contribution of mitochondrial proton leak to skeletal muscle respiration and to standard metabolic rate. *Am J Physiol Physiol*. 1996;271(4):C1380–C1389.
45 Brand MD, Esteves TC. Physiological functions of the mitochondrial uncoupling proteins UCP2 and UCP3. *Cell Metab*. 2005;2(2):85–93.
46 Bertholet AM, Chouchani ET, Kazak L, et al. H+ transport is an integral function of the mitochondrial ADP/ATP carrier. *Nature*. 2019;571(7766):515–520.
47 Brand MD, Pakay JL, Ocloo A, et al. The basal proton conductance of mitochondria depends on adenine nucleotide translocase content. *Biochem J*. 2005;392(2):353–362.
48 Lapuente-Brun E, Moreno-Loshuertos R, Acin-Perez R, et al. Supercomplex assembly determines electron flux in the mitochondrial electron transport chain. *Science*. 2013;340(6140):1567–1570.
49 Greggio C, Jha P, Kulkarni SS, et al. Enhanced respiratory chain supercomplex formation in response to exercise in human skeletal muscle. *Cell Metab*. 2017;25(2):301–311.

50 Geidenstam N, Al-Majdoub M, Ekman M, Spégel P, Ridderstråle M. Metabolite profiling of obese individuals before and after a one year weight loss program. *Int J Obes*. 2017;41(9):1369–1378.
51 Stroeve JHM, Saccenti E, Bouwman J, et al. Weight loss predictability by plasma metabolic signatures in adults with obesity and morbid obesity of the DiOGenes study. *Obesity (Silver Spring)*. 2016;24(2):379–388.
52 Piccolo BD, Keim NL, Fiehn O, Adams SH, Van Loan MD, Newman JW. Habitual physical activity and plasma metabolomic patterns distinguish individuals with low vs. high weight loss during controlled energy restriction. *J Nutr*. 2015;145(4):681–690.
53 Tulipani S, Griffin J, Palau-Rodriguez M, et al. Metabolomics-guided insights on bariatric surgery versus behavioral interventions for weight loss. *Obesity (Silver Spring)*. 2016;24(12):2451–2466.
54 Ducker GS, Rabinowitz JD. One-carbon metabolism in health and disease. *Cell Metab*. 2017;25(1):27–42.
55 Yang M, Vousden KH. Serine and one-carbon metabolism in cancer. *Nat Rev Cancer*. 2016;16(10):650–662.
56 Song J-W, Lam SM, Fan X, et al. Omics-driven systems interrogation of metabolic dysregulation in COVID-19 pathogenesis. *Cell Metab*. 2020;32(2):188–202.
57 Atkinson DE, Walton GM. Adenosine triphosphate conservation in metabolic regulation: rat liver citrate cleavage enzyme. *J Biol Chem*. 1967;242(13):3239–3241.
58 Larsen S, Nielsen J, Hansen CN, et al. Biomarkers of mitochondrial content in skeletal muscle of healthy young human subjects. *J Physiol*. 2012;590(14):3349–3360.
59 Hanada K. Serine palmitoyltransferase, a key enzyme of sphingolipid metabolism. *Biochim Biophys Acta*. 2003;1632(1–3):16–30.
60 Bergman BC, Brozinick JT, Strauss A, et al. Muscle sphingolipids during rest and exercise: a C18: 0 signature for insulin resistance in humans. *Diabetologia*. 2016;59(4):785–798.
61 Chung JO, Koutsari C, Blachnio-Zabielska AU, Hames KC, Jensen MD. Intramyocellular ceramides: subcellular concentrations and fractional de novo synthesis in postabsorptive humans. *Diabetes*. 2017;66(8):2082–2091.
62 Li Z, Zhang H, Liu J, et al. Reducing plasma membrane sphingomyelin increases insulin sensitivity. *Mol Cell Biol*. 2011;31(20):4205–4218.
63 Eisinger K, Liebisch G, Schmitz G, Aslanidis C, Krautbauer S, Buechler C. Lipidomic analysis of serum from high fat diet induced obese mice. *Int J Mol Sci*. 2014;15(2):2991–3002.
64 Jayedi A, Soltani S, Zargar MS, Khan TA, Shab-Bidar S. Central fatness and risk of all cause mortality: systematic review and dose-response meta-analysis of 72 prospective cohort studies. *BMJ*. 2020;370:m3324.
65 Arner P. Differences in lipolysis between human subcutaneous and omental adipose tissues. *Ann Med*. 1995;27(4):435–438.
66 Preis SR, Massaro JM, Robins SJ, et al. Abdominal subcutaneous and visceral adipose tissue and insulin resistance in the Framingham heart study. *Obesity (Silver Spring)*. 2010;18(11):2191–2198.
67 Rebuffé-Scrive M, Andersson B, Olbe L, Björntorp P. Metabolism of adipose tissue in intraabdominal depots of nonobese men and women. *Metabolism*. 1989;38(5):453–458.
68 Tchernof A, Bélanger C, Morisset A-S, et al. Regional differences in adipose tissue metabolism in women: minor effect of obesity and body fat distribution. *Diabetes*. 2006;55(5):1353–1360.
69 Nicklas BJ, Rogus EM, Colman EG, Goldberg AP. Visceral adiposity, increased adipocyte lipolysis, and metabolic dysfunction in obese postmenopausal women. *Am J Physiol Metab*. 1996;270(1):E72–E78.
70 Bergman BC, Goodpaster BH. Exercise and muscle lipid content, composition, and localization: influence on muscle insulin sensitivity. *Diabetes*. 2020;69(5):848–858.
71 Curioni CC, Lourenco PM. Long-term weight loss after diet and exercise: a systematic review. *Int J Obes*. 2005;29(10):1168–1174.
72 Avenell A, Brown TJ, McGee MA, et al. What interventions should we add to weight reducing diets in adults with obesity? A systematic review of randomized controlled trials of adding drug therapy, exercise, behaviour therapy or combinations of these interventions. *J Hum Nutr Diet*. 2004;17(4):293–316.
73 Foster-Schubert KE, Alfano CM, Duggan CR, et al. Effect of diet and exercise, alone or combined, on weight and body composition in overweight-to-obese postmenopausal women. *Obesity (Silver Spring)*. 2012;20(8):1628–1638.
74 Phillips SM, Joyner MJ. Out-running 'bad'diets: beyond weight loss there is clear evidence of the benefits of physical activity. *Br J Sports Med*. 2019;53(14):854–855.
75 Johns DJ, Hartmann-Boyce J, Jebb SA, Aveyard P, Group BWMR. Diet or exercise interventions vs combined behavioral weight management programs: a systematic review and meta-analysis of direct comparisons. *J Acad Nutr Diet*. 2014;114(10):1557–1568.
76 Sparks LM. Exercise training response heterogeneity: physiological and molecular insights. *Diabetologia*. 2017;60(12):2329–2336.
77 Thomas DM, Bouchard C, Church T, et al. Why do individuals not lose more weight from an exercise intervention at a defined dose? An energy balance analysis. *Obes Rev*. 2012;13(10):835–847.
78 Ross R, Dagnone D, Jones PJH, et al. Reduction in obesity and related comorbid conditions after diet-induced weight loss or exercise-induced weight loss in men: a randomized, controlled trial. *Ann Intern Med*. 2000;133(2):92–103.
79 Colleluori G, Aguirre L, Phadnis U, et al. Aerobic plus resistance exercise in obese older adults improves muscle protein synthesis and preserves myocellular quality despite weight loss. *Cell Metab*. 2019;30(2):261–273.
80 Chomentowski P, Dubé JJ, Amati F, et al. Moderate exercise attenuates the loss of skeletal muscle mass that occurs with intentional caloric restriction–induced weight loss in older, overweight to obese adults. *J Gerontol A Biol Sci Med Sci*. 2009;64(5):575–580.
81 Cermak NM, Snijders T, McKay BR, et al. Eccentric exercise increases satellite cell content in type II muscle fibers. *Med Sci Sport Exerc*. 2013;45(2):230–237.
82 Figueiredo VC, Caldow MK, Massie V, Markworth JF, Cameron-Smith D, Blazevich AJ. Ribosome biogenesis adaptation in resistance training-induced human skeletal muscle hypertrophy. *Am J Physiol Metab*. 2015;309(1):E72–E83.
83 Starritt EC, Angus D, Hargreaves M. Effect of short-term training on mitochondrial ATP production rate in human skeletal muscle. *J Appl Physiol*. 1999;86(2):450–454.
84 Barres R, Yan J, Egan B, et al. Acute exercise remodels promoter methylation in human skeletal muscle. *Cell Metab*. 2012;15(3):405–411.

Figure S1. (a) Average daily steps differed between DR and DS women at BL and throughout the exercise intervention, (n=10). **(b and c)** Substrate utilization at rest, (n=10). **(b)** Calculated absolute rates of carbohydrate (CHO) and fatty acid (FA) oxidation at rest. **(c)** Relative contribution of substrate utilization to energy expenditure at rest. **(d-h)** Measurements during a graded exercise test, (n=10). **(d)** VO_2, **(e)** Rating of perceived exertion (RPE) (using the Borg) and, **(f)** Muscle-specific cost of transport (amount of energy required to move 1 meter) did not differ between DS and DR women with obesity. **(g)** Calculated carbohydrate (CHO) and fatty acid (FA) oxidation. **(h)** Relative contribution of substrate utilization to energy expenditure during a graded exercise test. **(i)** *Vastus lateral*is CSA tended to be lower in DR skeletal muscle (P=0.062) (n=8 DS, n=7 DR). A two-way ANOVA for repeated-measures was used to analyse exercise and diet sensitivity group differences. † Main effect of DS *vs*. DR (P<0.05). Holm-Sidak post hoc tests were performed for multiple comparisons. *P<0.05. All values are presented as means±SD.

Figure S2. **(a)** Respiratory flux per citrate synthase activity (per mg) of *vastus lateral*is at baseline (BL), after 6 weeks of exercise training (PET), (n=9 DS, n=7 DR). **(b)** H_2O_2 emissions per mg *vastus lateral*is, (n=7). **(c-e)** Cellular respiration is increased in DR myotubes following exercise training. Primary myotubes were analyzed using a Seahorse XFe96 analyzer (Agilent) with serial injections of oligomycin (Oligo), FCCP, rotenone with antimycin A (Rot&AA), and monensin (Mon). **(c)** Quantification of the indicated parameter of respiration (main text figure 3e). **(d)** ECAR of primary myotubes. **(e)** Cellular bioenergetic analyses of the data presented in **a&b.** The rate of ATP produced by OXPHOS and glycolysis (J_{ATPox} and $J_{ATPglyc}$ respectively) were calculated following the Mookerjee *et al.*, 2017 method (see STAR methods). A two-way ANOVA for repeated-measures was used to analyse exercise and diet sensitivity group differences. † Main effect of DS *vs*. DR (p<0.05), ‡ Main effect of exercise (P<0.05). Holm-Sidak post hoc tests were performed for multiple comparisons. *P<0.05, **P<0.01 ***P<0.001. All values are presented as means±SD, (n=9).

Figure S3. Primary myotubes supercomplex analyses. Analysis of ETC supercomplex levels by BN-PAGE**.** Intensities of complex I, III and IV related SC relative to complex II in primary myotubes from DR and DS individuals before (BL) and after exercise training (PET). A two-way ANOVA for repeated-measures was used to analyse exercise and diet sensitivity group differences. † Main effect of DS *vs*. DR (P<0.05), ‡ Main effect of exercise (P<0.05). Holm-Sidak post hoc tests were performed for multiple comparisons. *P<0.05. All values are presented as means±SD, (n=8).

Figure S4. Distance correlation network for muscle serine/PE and sphingolipids. Signed distance correlation analysis of serine and O-phosphorylethanolamine (PE) with sphingolipids showing major change between groups. Shown are partners with distance correlation > 0.7; P<0.02, (n=5).

Figure S5. Comparison of distance correlation networks for metabolites. **(a)** *Vastus lateralis* muscle metabolite profiles at baseline (BL) and post-exercise training (PET). Shown are

correlation > 0.6, P< 0.01, (n=9 DS, n=8 DR). **(b)** Comparison of distance correlation networks for plasma metabolites. Shown are correlation > 0.8, P< 0.01, (n=10).

Figure S6. Distance correlation networks of *vastus lateralis* from DS and DR women at baseline (BL) and post-exercise training (PET) **(**profiles at correlation > 0.8, P< 0.01), (n=9 DS, n=8 DR).

Figure S7. Distance correlation network for plasma sample metabolomics in four groups. Shown are positive (black) and negative (red) correlations (profiles at correlation >0.8, P<0.02), (n=10).

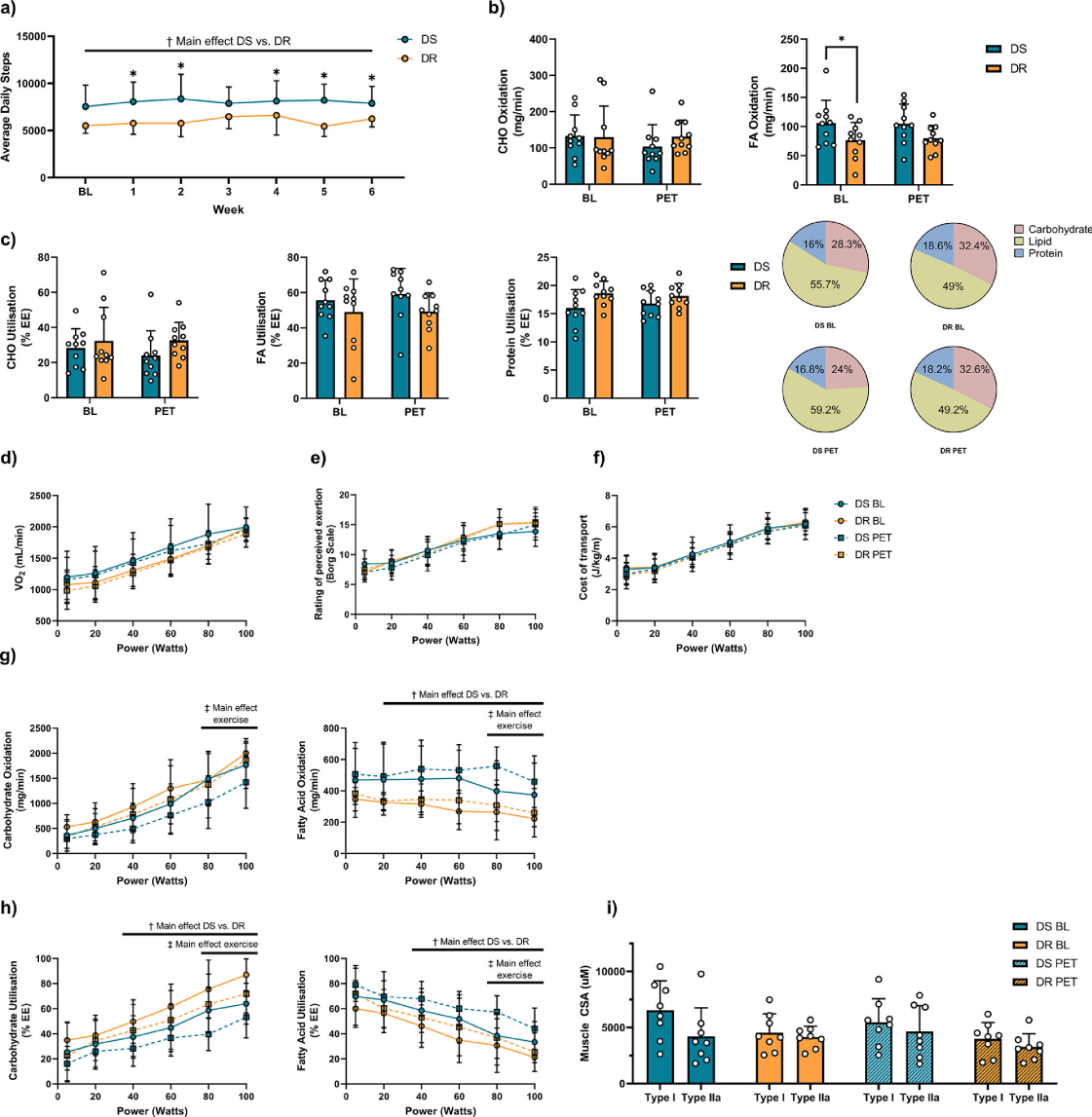
a)
† Main effect DS vs. DR
DS
DR
Average Daily Steps
Week
BL
b)
CHO Oxidation (mg/min)
FA Oxidation (mg/min)
BL
PET
c)
CHO Utilisation (% EE)
FA Utilisation (% EE)
Protein Utilisation (% EE)
Carbohydrate
Lipid
Protein
16%
28.3%
55.7%
DS BL
18.6%
32.4%
49%
DR BL
16.8%
24%
59.2%
DS PET
18.2%
32.6%
49.2%
DR PET
d)
VO2 (mL/min)
Power (Watts)
e)
Rating of perceived exertion (Borg Scale)
f)
Cost of transport (J/kg/m)
DS BL
DR BL
DS PET
DR PET
g)
‡ Main effect exercise
Carbohydrate Oxidation (mg/min)
Fatty Acid Oxidation (mg/min)
h)
Carbohydrate Utilisation (% EE)
Fatty Acid Utilisation (% EE)
i)
Muscle CSA (uM)
Type I
Type IIa

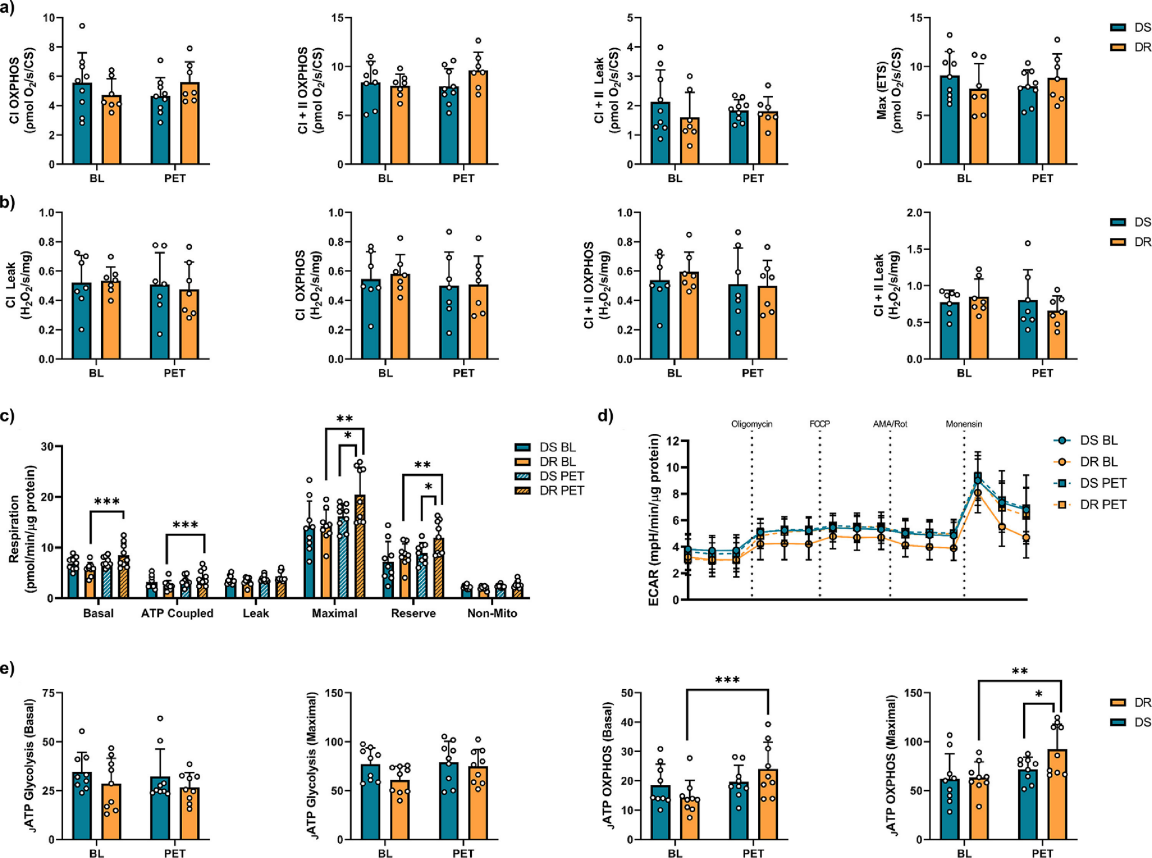
a)
CI OXPHOS (pmol O2/s/CS)
CI + II OXPHOS (pmol O2/s/CS)
CI + II Leak (pmol O2/s/CS)
Max (ETS) (pmol O2/s/CS)
BL
PET
DS
DR
b)
CI Leak (H2O2/s/mg)
CI OXPHOS (H2O2/s/mg)
CI + II OXPHOS (H2O2/s/mg)
CI + II Leak (H2O2/s/mg)
c)
Respiration (pmol/min/µg protein)
Basal
ATP Coupled
Leak
Maximal
Reserve
Non-Mito
DS BL
DR BL
DS PET
DR PET
d)
ECAR (mpH/min/µg protein)
Oligomycin
FCCP
AMA/Rot
Monensin
e)
JATP Glycolysis (Basal)
JATP Glycolysis (Maximal)
JATP OXPHOS (Basal)
JATP OXPHOS (Maximal)

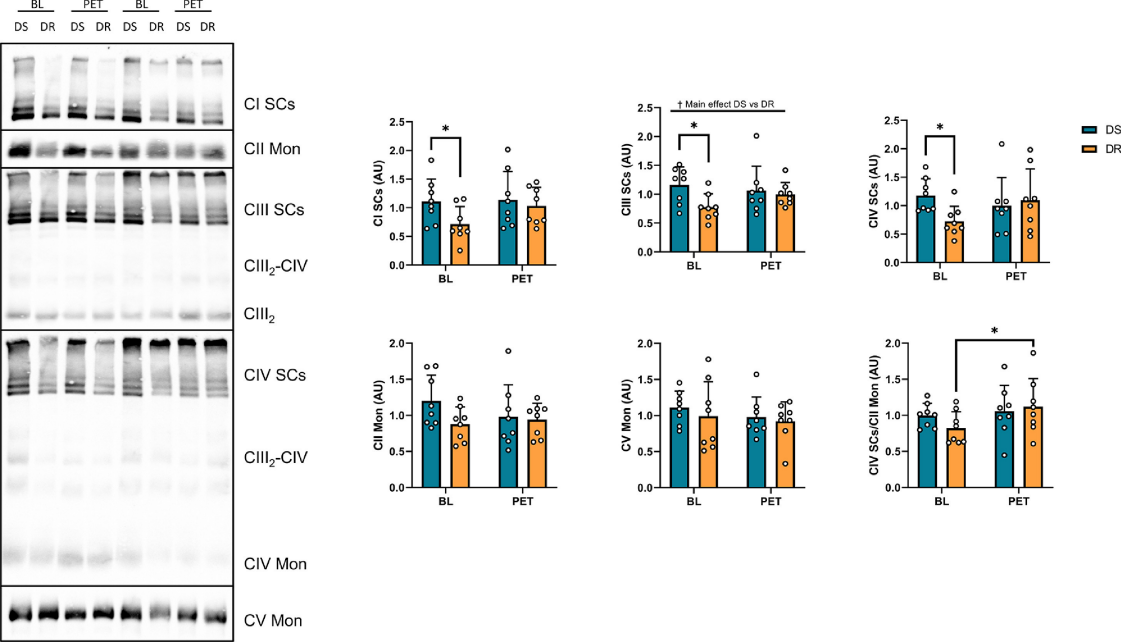
BL
PET
BL
PET
DS DR DS DR DS DR DS DR
CI SCs
CII Mon
CIII SCs
CIII2-CIV
CIII2
CIV SCs
CIII2-CIV
CIV Mon
CV Mon
CI SCs (AU)
CII Mon (AU)
CIII SCs (AU)
† Main effect DS vs DR
CIV SCs (AU)
CV Mon (AU)
CIV SCs/CII Mon (AU)
BL
PET
DS
DR

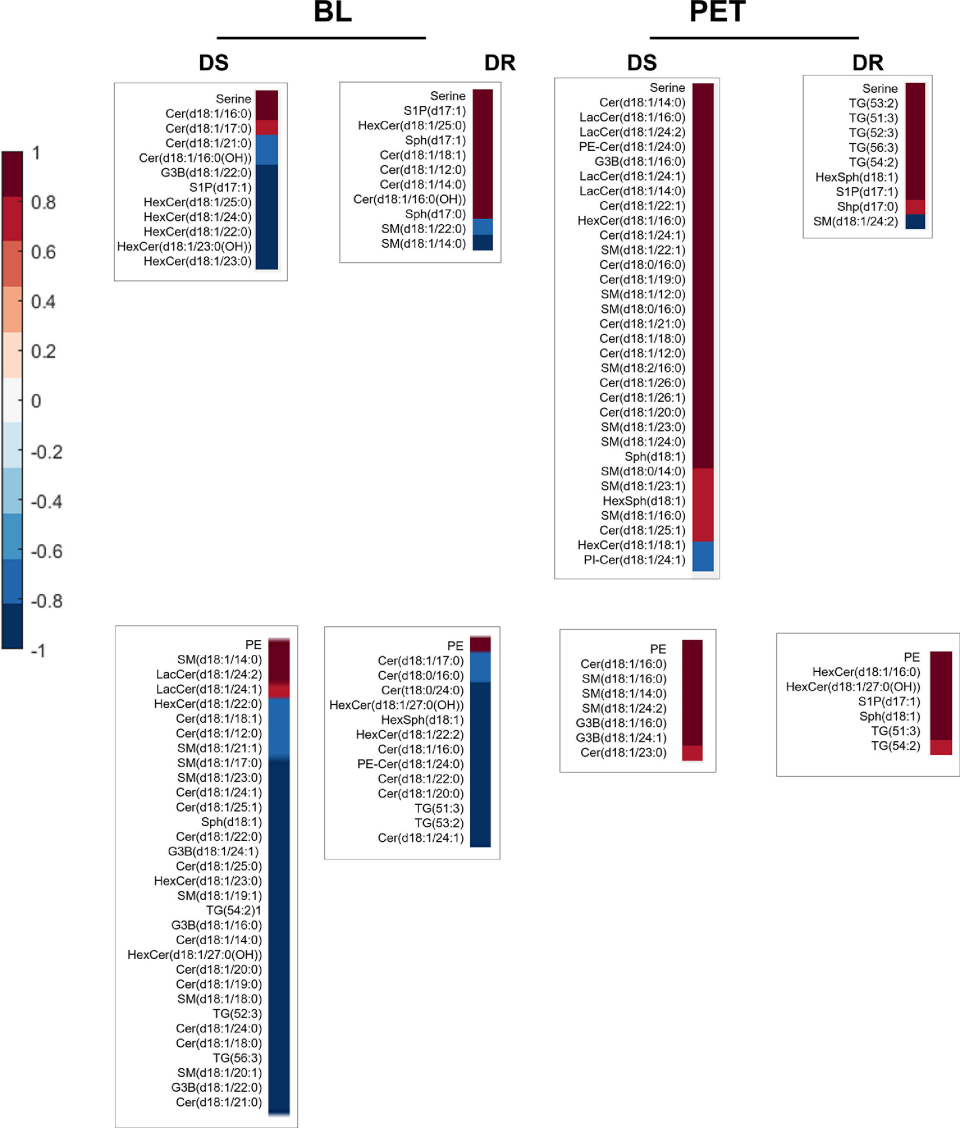
BL
PET
DS
DR
DS
DR
1
0.8
0.6
0.4
0.2
0
-0.2
-0.4
-0.6
-0.8
-1
Serine
Cer(d18:1/16:0)
Cer(d18:1/17:0)
Cer(d18:1/21:0)
Cer(d18:1/16:0(OH))
G3B(d18:1/22:0)
S1P(d17:1)
HexCer(d18:1/25:0)
HexCer(d18:1/24:0)
HexCer(d18:1/22:0)
HexCer(d18:1/23:0(OH))
HexCer(d18:1/23:0)
Serine
S1P(d17:1)
HexCer(d18:1/25:0)
Sph(d17:1)
Cer(d18:1/18:1)
Cer(d18:1/12:0)
Cer(d18:1/14:0)
Cer(d18:1/16:0(OH))
Sph(d17:0)
SM(d18:1/22:0)
SM(d18:1/14:0)
Serine
Cer(d18:1/14:0)
LacCer(d18:1/16:0)
LacCer(d18:1/24:2)
PE-Cer(d18:1/24:0)
G3B(d18:1/16:0)
LacCer(d18:1/24:1)
LacCer(d18:1/14:0)
Cer(d18:1/22:1)
HexCer(d18:1/16:0)
Cer(d18:1/24:1)
SM(d18:1/22:1)
Cer(d18:0/16:0)
Cer(d18:1/19:0)
SM(d18:1/12:0)
SM(d18:0/16:0)
Cer(d18:1/21:0)
Cer(d18:1/18:0)
Cer(d18:1/12:0)
SM(d18:2/16:0)
Cer(d18:1/26:0)
Cer(d18:1/26:1)
Cer(d18:1/20:0)
SM(d18:1/23:0)
SM(d18:1/24:0)
Sph(d18:1)
SM(d18:0/14:0)
SM(d18:1/23:1)
HexSph(d18:1)
SM(d18:1/16:0)
Cer(d18:1/25:1)
HexCer(d18:1/18:1)
PI-Cer(d18:1/24:1)
Serine
TG(53:2)
TG(51:3)
TG(52:3)
TG(56:3)
TG(54:2)
HexSph(d18:1)
S1P(d17:1)
Shp(d17:0)
SM(d18:1/24:2)
PE
SM(d18:1/14:0)
LacCer(d18:1/24:2)
LacCer(d18:1/24:1)
HexCer(d18:1/22:0)
Cer(d18:1/18:1)
Cer(d18:1/12:0)
SM(d18:1/21:1)
SM(d18:1/17:0)
SM(d18:1/23:0)
Cer(d18:1/24:1)
Cer(d18:1/25:1)
Sph(d18:1)
Cer(d18:1/22:0)
G3B(d18:1/24:1)
Cer(d18:1/25:0)
HexCer(d18:1/23:0)
SM(d18:1/19:1)
TG(54:2)1
G3B(d18:1/16:0)
Cer(d18:1/14:0)
HexCer(d18:1/27:0(OH))
Cer(d18:1/20:0)
Cer(d18:1/19:0)
SM(d18:1/18:0)
TG(52:3)
Cer(d18:1/24:0)
Cer(d18:1/18:0)
TG(56:3)
SM(d18:1/20:1)
G3B(d18:1/22:0)
Cer(d18:1/21:0)
PE
Cer(d18:1/17:0)
Cer(d18:0/16:0)
Cer(t18:0/24:0)
HexCer(d18:1/27:0(OH))
HexSph(d18:1)
HexCer(d18:1/22:2)
Cer(d18:1/16:0)
PE-Cer(d18:1/24:0)
Cer(d18:1/22:0)
Cer(d18:1/20:0)
TG(51:3)
TG(53:2)
Cer(d18:1/24:1)
PE
Cer(d18:1/16:0)
SM(d18:1/16:0)
SM(d18:1/14:0)
SM(d18:1/24:2)
G3B(d18:1/16:0)
G3B(d18:1/24:1)
Cer(d18:1/23:0)
PE
HexCer(d18:1/16:0)
HexCer(d18:1/27:0(OH))
S1P(d17:1)
Sph(d18:1)
TG(51:3)
TG(54:2)

a)

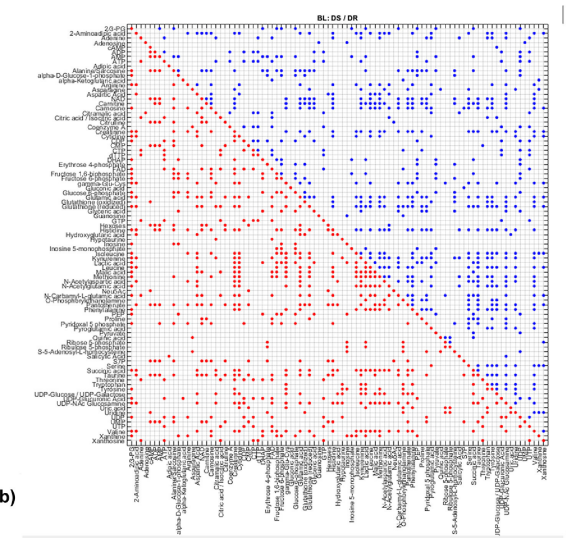

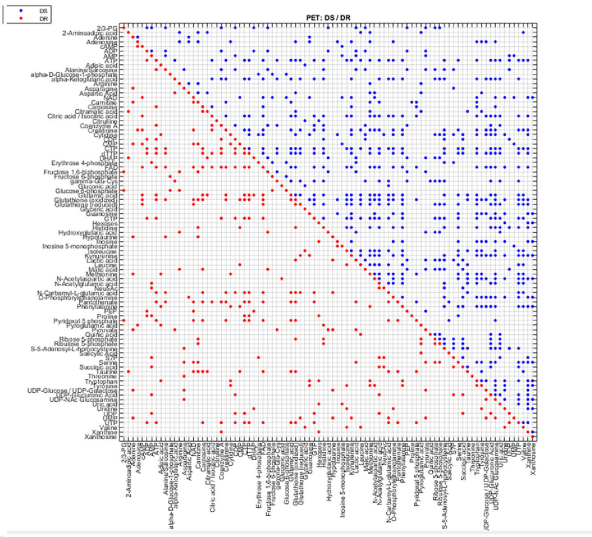

b)

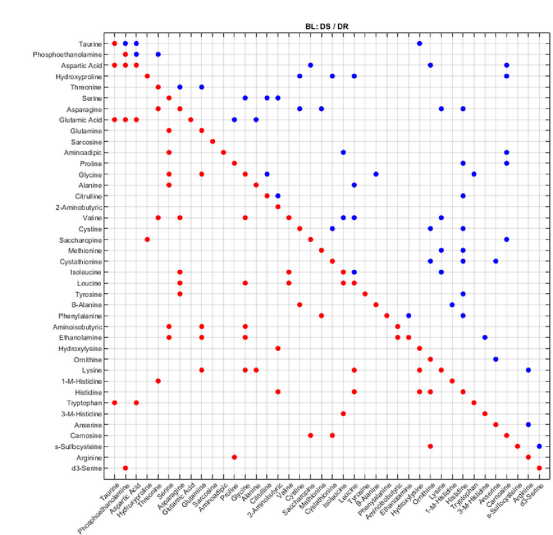

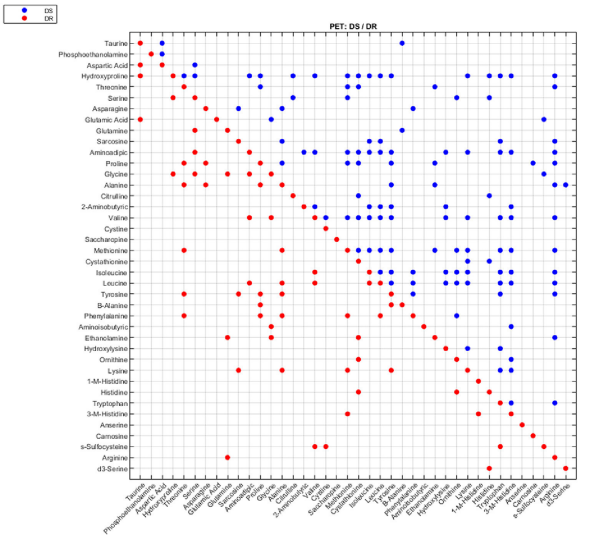

DS BL

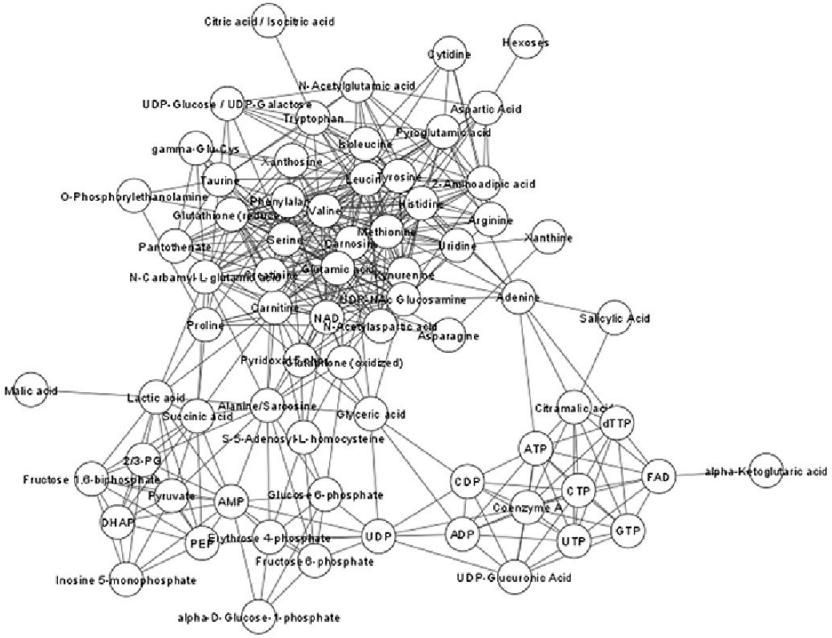

DR BL

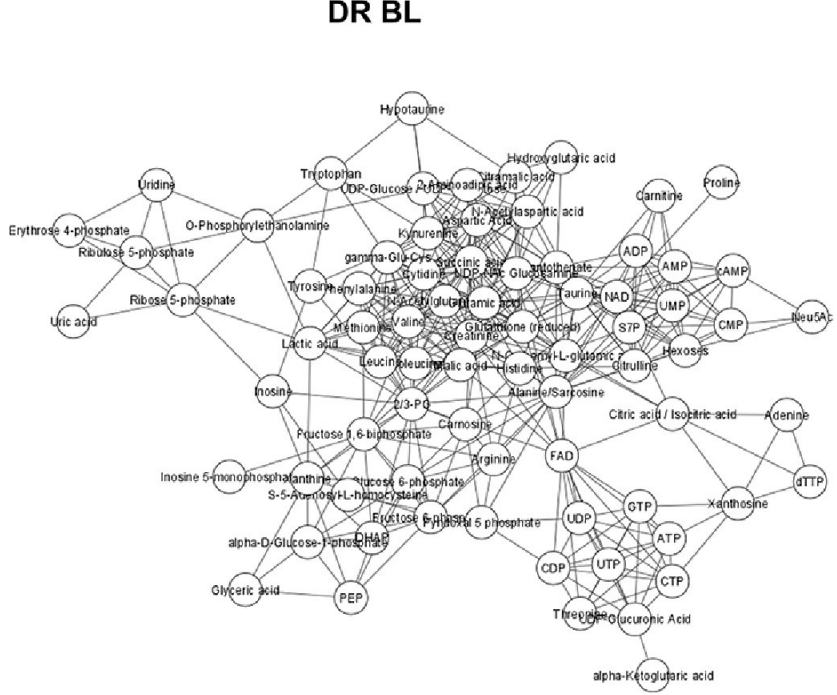

DS PET

DR PET

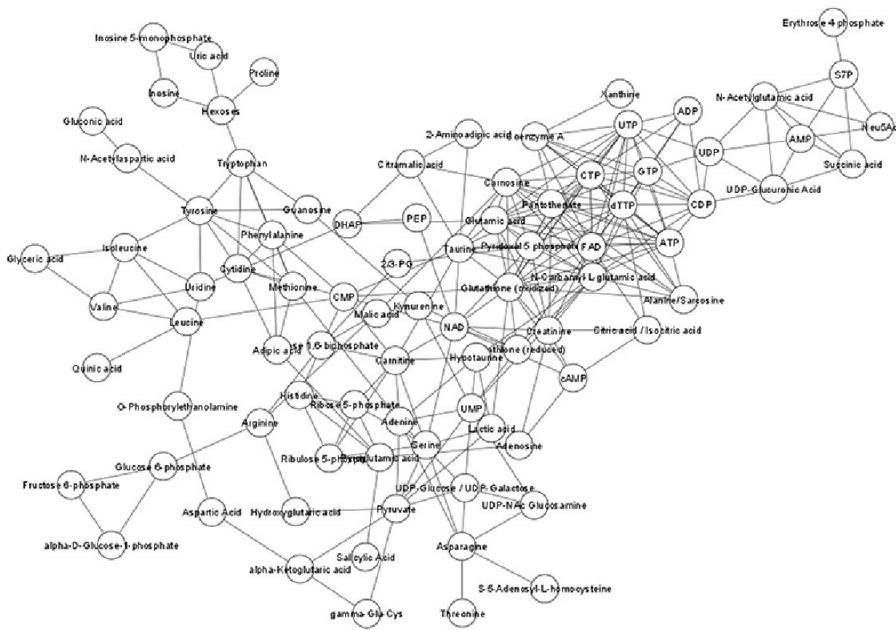

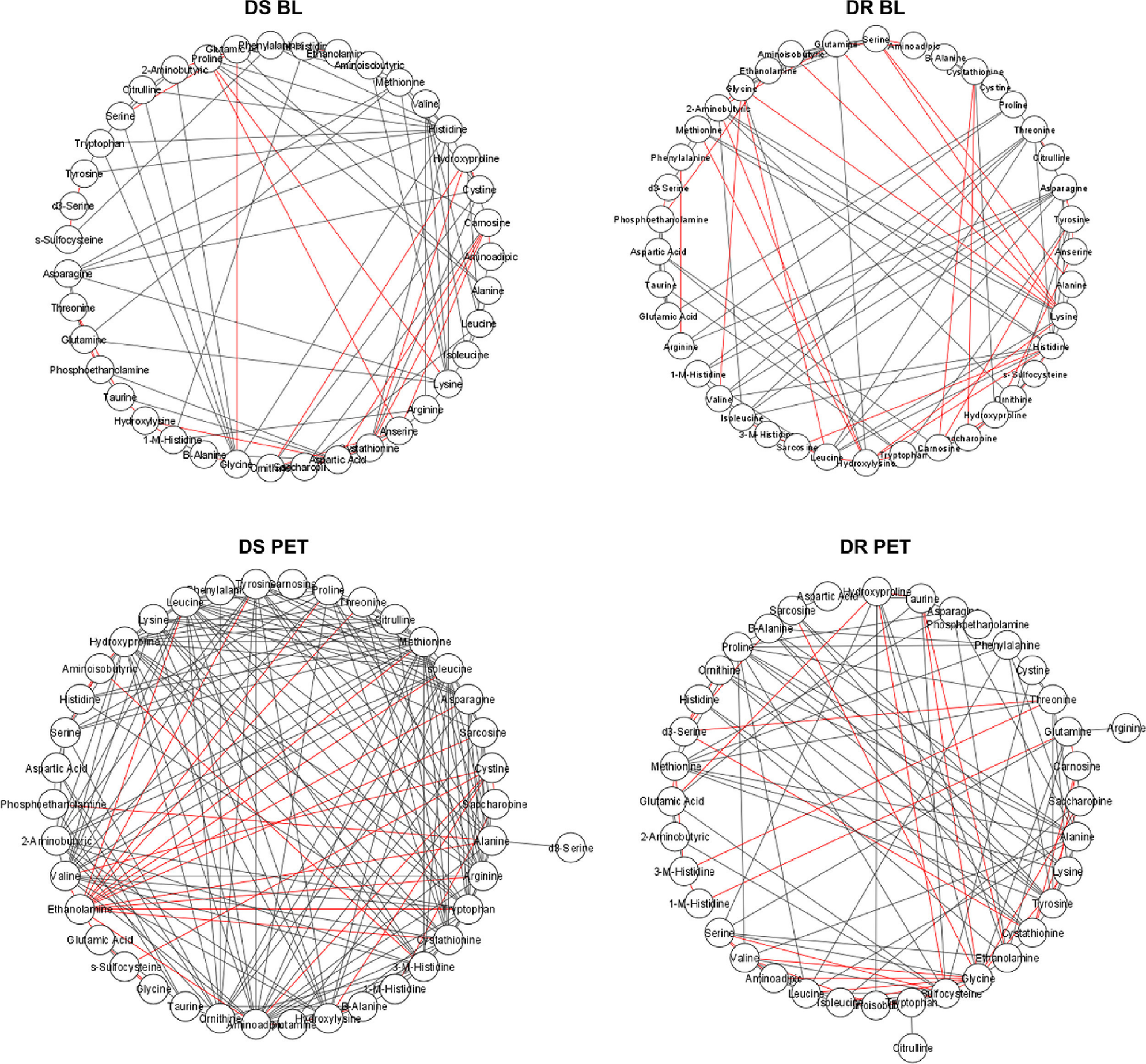
DS BL
Glutamic Ac
Phenylalanine
Histidine
Proline
Ethanolamine
2-Aminobutyric
Aminoisobutyric
Citrulline
Methionine
Serine
Valine
Tryptophan
Histidine
Tyrosine
Hydroxyproline
d3-Serine
Cystine
s-Sulfocysteine
Carnosine
Asparagine
Aminoadipic
Threonine
Alanine
Glutamine
Leucine
Phosphoethanolamine
Isoleucine
Taurine
Lysine
Hydroxylysine
Arginine
1-M-Histidine
Anserine
B-Alanine
Cystathionine
Glycine
Aspartic Acid
DR BL
Glutamine
Serine
Aminoisobutyric
Aminoadipic
B-Alanine
Ethanolamine
Cystathionine
Glycine
Cystine
2-Aminobutyric
Proline
Methionine
Threonine
Phenylalanine
Citrulline
d3-Serine
Asparagine
Phosphoethanolamine
Tyrosine
Aspartic Acid
Anserine
Taurine
Alanine
Glutamic Acid
Lysine
Arginine
Histidine
1-M-Histidine
s-Sulfocysteine
Valine
Ornithine
Isoleucine
Hydroxyproline
3-M-Histidine
Sarcosine
Leucine
Tryptophan
Carnosine
Hydroxylysine
DS PET
Tyrosine
Carnosine
Phenylalanine
Proline
Leucine
Threonine
Lysine
Citrulline
Hydroxyproline
Methionine
Aminoisobutyric
Isoleucine
Histidine
Asparagine
Serine
Sarcosine
Aspartic Acid
Cystine
Phosphoethanolamine
Saccharopine
2-Aminobutyric
Alanine
d3-Serine
Valine
Arginine
Ethanolamine
Tryptophan
Glutamic Acid
Cystathionine
s-Sulfocysteine
3-M-Histidine
Glycine
1-M-Histidine
Taurine
B-Alanine
Ornithine
Hydroxylysine
Aminoadipic
Glutamine
DR PET
Aspartic Acid
Hydroxyproline
Taurine
Sarcosine
Asparagine
B-Alanine
Phosphoethanolamine
Proline
Phenylalanine
Ornithine
Cystine
Histidine
Threonine
d3-Serine
Glutamine
Arginine
Methionine
Carnosine
Glutamic Acid
Saccharopine
2-Aminobutyric
Alanine
3-M-Histidine
Lysine
1-M-Histidine
Tyrosine
Serine
Cystathionine
Valine
Ethanolamine
Aminoadipic
Glycine
Leucine
Isoleucine
Sulfocysteine
Tryptophan
Citrulline

Table S1. Clinical factors associated with high vs. low capacity for diet-induced weight loss.

Variable	DS	DR	P-value
n	114	114	
Age (years)	46.3 ± 8.5	45.8 ± 8.2	-
Height (cm)	165.0 ± 6.3	165.0 ± 5.7	-
Weight (kg)	114.0 ± 18.2	114.5 ± 17.9	-
BMI (kg/m^2)	41.87 ± 6.06	42.24 ± 5.78	-
% Weight loss	11.88 ± 1.35	6.59 ± 1.18*	<0.001
Systolic BP (mmHg)	137 ± 17	128 ± 17*	<0.001
Diastolic BP (mmHg)	84 ± 9	81 ± 10*	<0.05
Waist Circumference	119.3 ± 14.6	115.5 ± 14.0	<0.05
ATP-III criteria for Metabolic Syndrome	3.34 ± 1.19	2.86 ± 1.30*	<0.01
Body composition by bioelectrical impedance			
Fat mass (kg)	54.7 ± 12.6	56.7 ± 12.1	0.21
Fat free mass (kg)	58.9 ± 7.3	57.8 ± 6.8	0.22
Total body water (kg)	43.1 ± 5.3	42.3 ± 5.0	0.25
Body fat (%)	47.7 ± 4.3	49.2 ± 3.5*	<0.01
Fasting blood biochemistry			
Glucose (mmol/L)	5.7 ± 1.3	5.7 ± 1.8	0.44
HbA1c (%)	5.6 ± 0.6	5.7 ± 1.0	0.25
Insulin (pmol/L)	106.0 ± 81.4	85.8 ± 45.6*	<0.05
HOMA-IR	3.89 ± 3.30	3.01 ± 2.23*	<0.05
HOMA-β	163.7 ± 114.5	151.8 ± 81.0	0.41
Triglycerides (mmol/L)	1.80 ± 0.73	1.59 ± 0.85*	<0.05
Total cholesterol (mmol/L)	4.93 ± 0.92	4.94 ± 1.07	0.91
HDL-cholesterol (mmol/L)	1.13 ± 0.27	1.29 ± 0.31*	<0.001
LDL cholesterol (mmol/L)	2.96 ± 0.87	2.93 ± 0.94	0.81
TSH (mIU/L)	2.04 ± 0.98	2.33 ± 1.11	<0.05

Free T3 (pmol/L)	4.46 ± 0.71	4.50 ± 0.77	0.66
Body composition by DEXA			
n	20	20	
Age (years)	53.81 ± 6.60	52.52 ± 7.81	-
Height (cm)	163.0 ± 5.7	161.7 ± 6.6	-
Body weight (kg)	98.4 ± 17.4	98.3 ± 17.4	-
BMI (kg/m^2)	36.9 ± 5.5	37.6 ± 6.3	-
Fat mass (kg)	45.9 ± 12.0	50.4 ± 12.5	0.24
Lean body mass (kg)	49.5 ± 5.6	45.1 ± 5.8*	<0.05
Body fat (%)	47.5 ± 4.1	52.3 ± 4.9*	<0.001
Android fat (%)	55.0 ± 5.9	56.7 ± 6.1	0.39
Gynoid fat (%)	48.5 ± 5.6	53.9 ± 5.6*	<0.01
Android/Gynoid fat	1.15 ± 0.17	1.06 ± 0.12	<0.05
Leg fat (%)	44.8 ± 5.6	53.6 ± 6.7*	<0.001
Leg fat (kg)	13.3 ± 4.5	17.6 ± 4.8*	<0.001
Leg lean mass (kg)	15.8 ± 1.2	14.9 ± 2.5	0.17

DS, diet-sensitive obesity; DR, diet-resistant obesity; BMI, body mass index; BP, blood pressure.

Full Western Blots

Figure 3

PGC1α

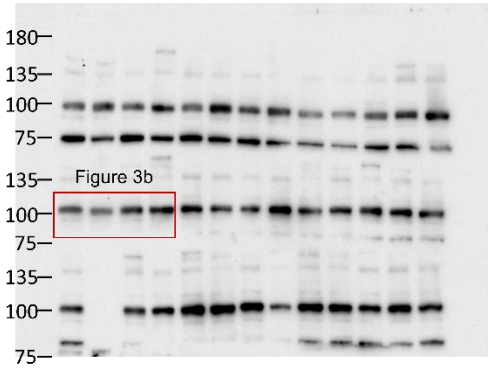

Vinculin

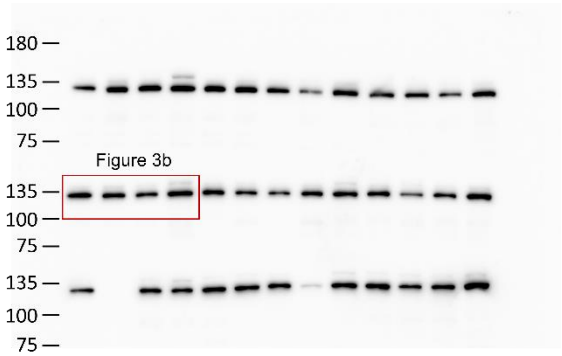

Figure 3

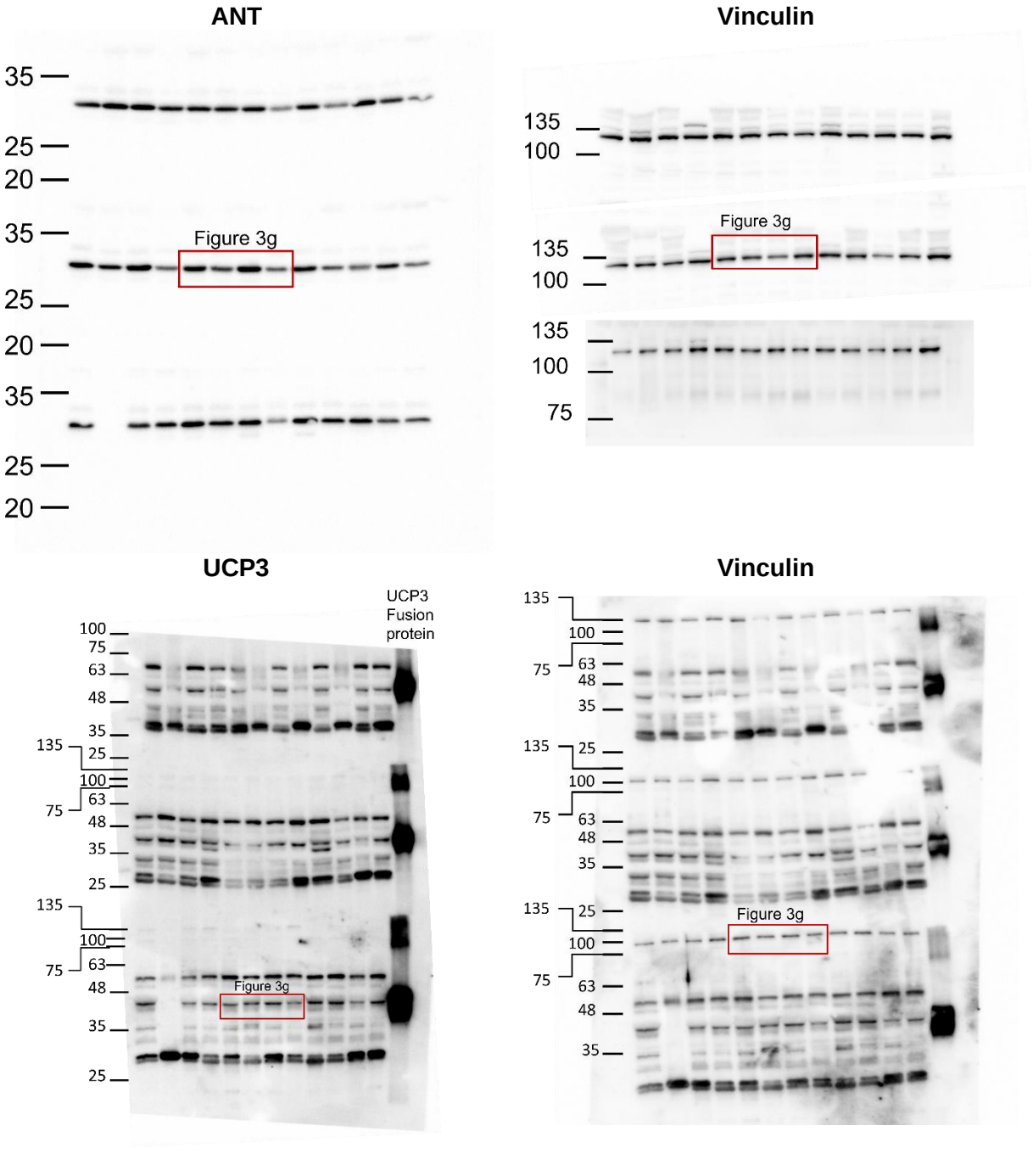
ANT
35
25
20
35
Figure 3g
25
20
35
25
20
Vinculin
135
100
Figure 3g
135
100
135
100
75
UCP3
UCP3
Fusion
protein
100
75
63
48
35
135
25
100
63
75
48
35
25
135
100
63
75
48
Figure 3g
35
25
Vinculin
135
100
75
63
48
35
135
25
100
75
63
48
35
135
25
Figure 3g
100
75
63
48
35

Figure 5

SPTLC1

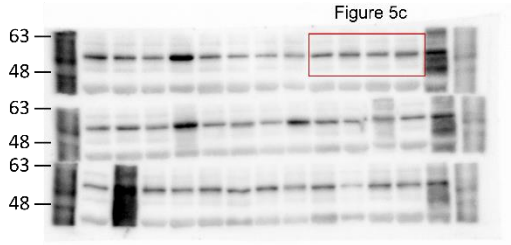

Vinculin

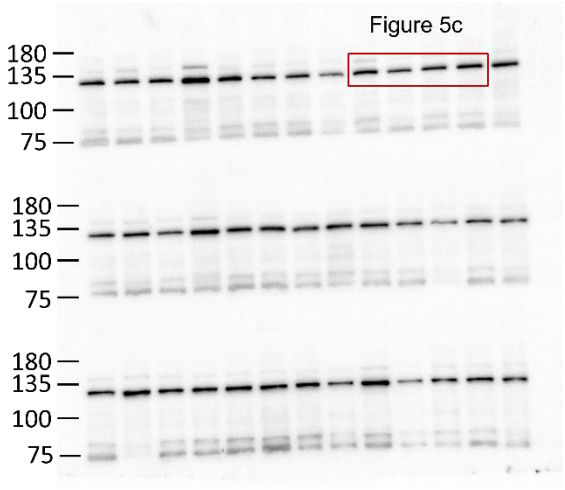

SPTLC2

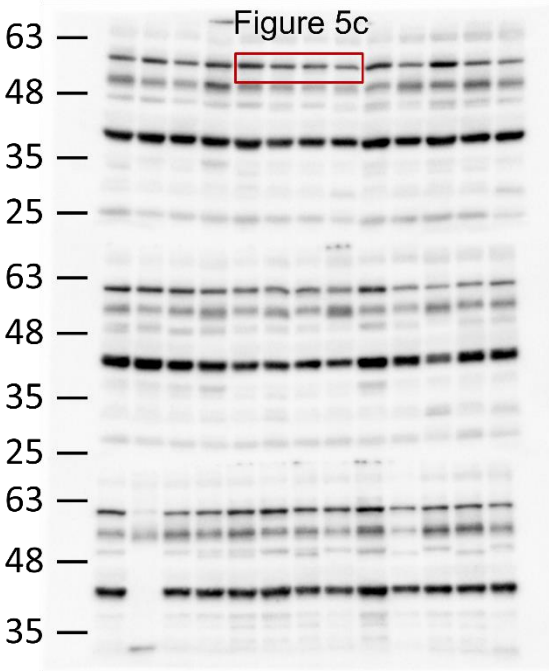

Vinculin

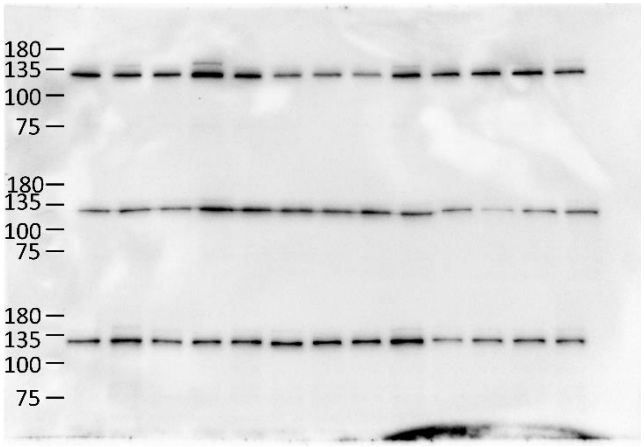

Full blots for BN-PAGE on skeletal muscle biopsies

Set 1 (presented figure 3h and 3i)

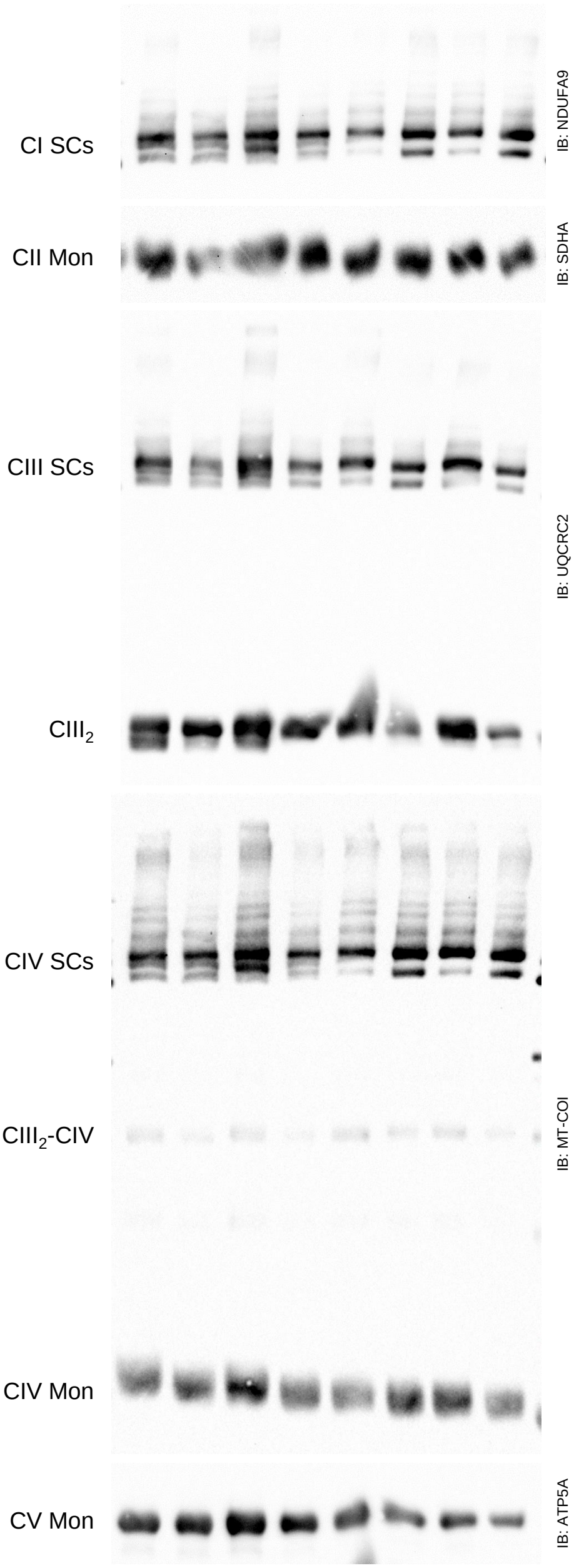

Set 2

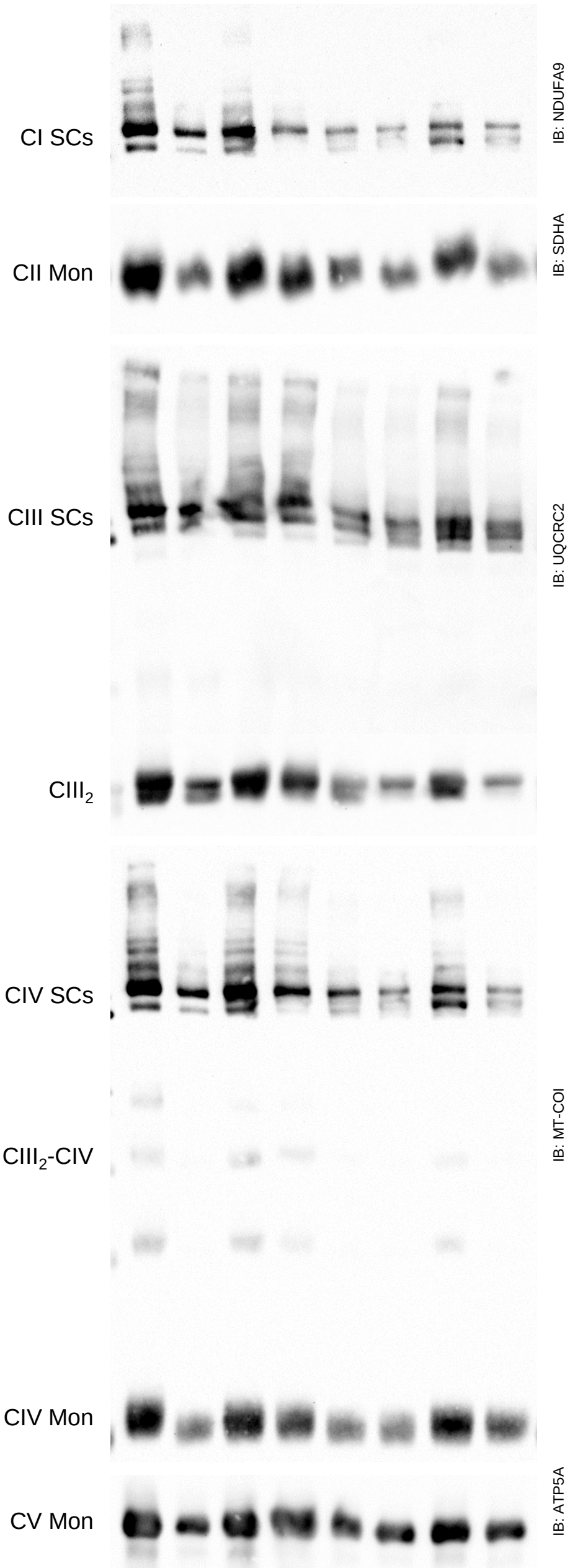

Set 3

CI SCs

IB: NDUFA9

CII Mon

IB: SDHA

CIII SCs

IB: UQCRC2

$CIII_2$

CIV SCs

IB: MT-COI

CIV Mon

CV Mon

IB: ATP5A

Set 4

CI SCs

IB: NDUFA9

CII Mon

CIII SCs

IB: UQCRC2

$CIII_2$

CIV SCs

IB: MT-COI

CIV Mon

CV Mon

IB: ATP5A

Full blots for BN-PAGE on primary myotubes

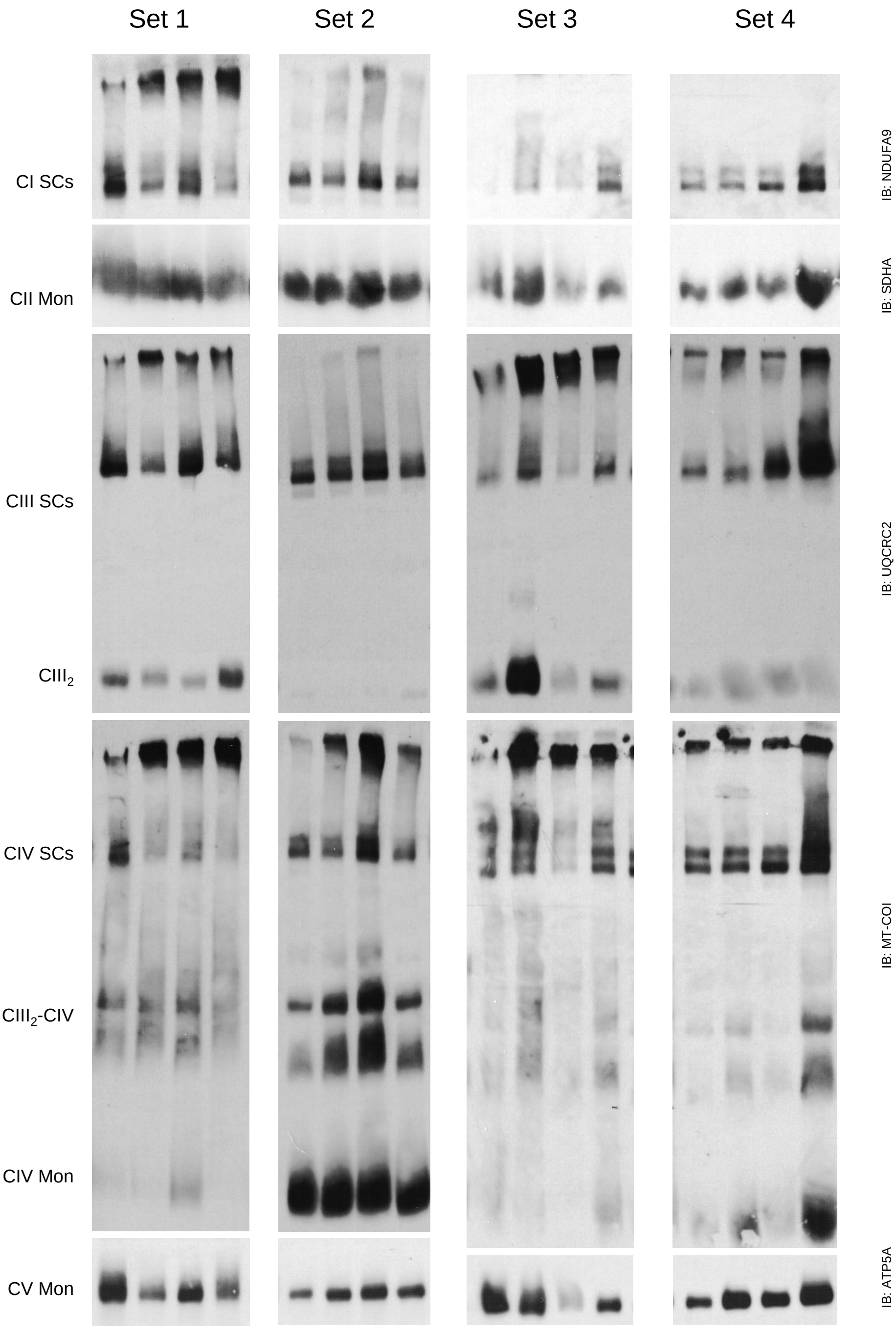

Set 5
(presented in Figure S3)

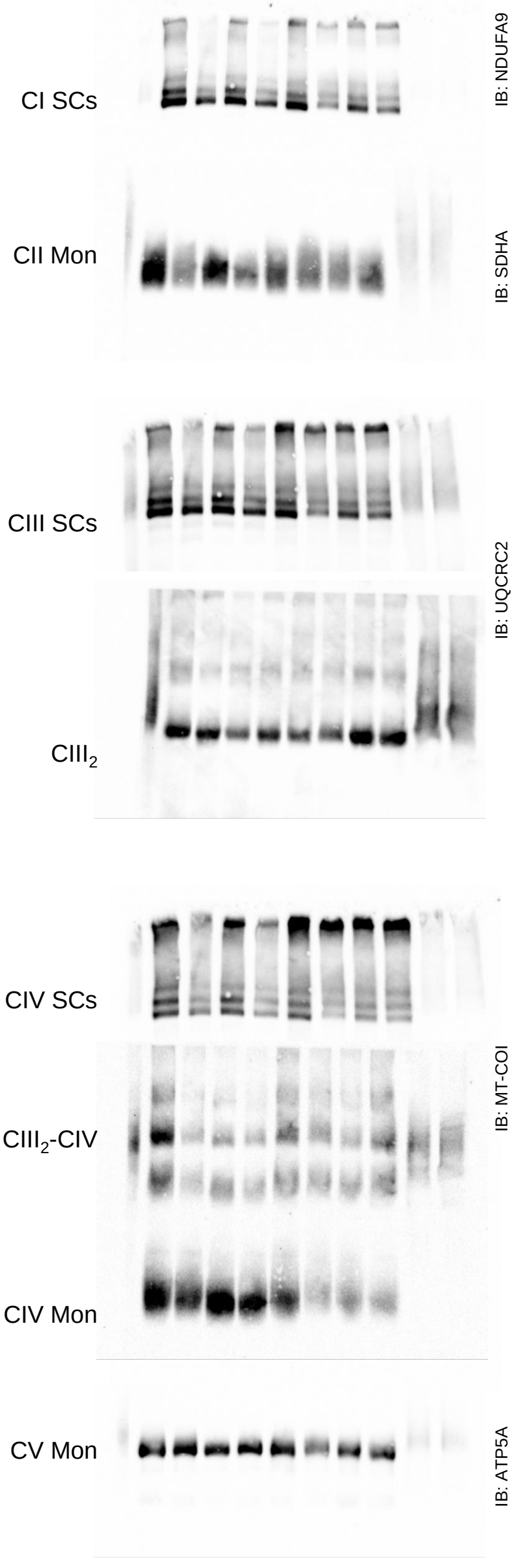

Set 6